fMRI Investigation of Cortical and Subcortical Networks in the Learning of Abstract and Effector-Specific Representations of Motor Sequences

Raju S. Bapi[1], K. P. Miyapuram[1], F. X. Graydon[2], K. Doya[3,4]

[1] Department of Computer and Information Sciences, University of Hyderabad, Hyderabad 500 046, India

[2] Brain Imaging Research Division, Dept of Psychiatry and Behavioral Neurosciences, Wayne State University School of Medicine, Detroit, MI, USA.

[3] Department of Computational Neurobiology, Computational Neuroscience Laboratories, Advanced Telecommunications Research International, Kyoto, Japan.

[4] Initial Research Project, Okinawa Institute of Science and Technology, Okinawa, Japan.

Abbreviated Title: Sequence Representations

Number of Figures: 7

Number of Tables: 4

Number of Words in Abstract: 247

Corresponding Author:

Dr. Raju S. Bapi

Dept of Computer and Information Sciences, University of Hyderabad,

Gachibowli, Hyderabad 500 046, India

Telephone Number: +91 40 23134014 (Work) / +91 40 24013032 (Home)

Fax Number: +91 40 23010780

Email: bapics@uohyd.ernet.in, bapiks@yahoo.co.in

Acknowledgments

This study was supported by grants from Japan Science and Technology Corporation under the ERATO and CREST schemes. We thank Richard Henson, Okihide Hikosaka, Hiroshi Imamizu, Mitsuo Kawato, and Hiroyuki Nakahara for helpful comments and Alex Harner for the experimental software. We thank anonymous reviewers for their suggestions for improving the manuscript. We thank Joe Gati, for the help in running the experiments and V. S. Chandrasekhar Pammi and Ahmed, UH for help with analysis.

ABSTRACT

A visuomotor sequence can be learned as a series of visuo-spatial cues or as a sequence of effector movements. Earlier imaging studies have revealed that a network of brain areas is activated in the course of motor sequence learning. However these studies do not address the question of the type of representation being established at various stages of visuomotor sequence learning. In an earlier behavioral study, we demonstrated that acquisition of visuo-spatial sequence representation enables rapid learning in the early stage and progressive establishment of somato-motor representation helps speedier execution by the late stage. We conducted functional magnetic resonance imaging (fMRI) experiments wherein subjects learned and practiced the same sequence alternately in *normal* and *rotated* settings. In one *rotated* setting (*visual*), subjects learned a new motor sequence in response to an identical sequence of visual cues as in *normal*. In another *rotated* setting (*motor*), the display sequence was altered as compared to *normal*, but the same sequence of effector movements were used to perform the sequence. Comparison of different *rotated* settings revealed analogous transitions both in the cortical and subcortical sites during visuomotor sequence learning — a transition of activity from parietal to parietal-premotor and then to premotor cortex and a concomitant shift was observed from anterior putamen to a combined activity in both anterior and posterior putamen and finally to posterior putamen. These results suggest a putative role for engagement of different cortical and subcortical networks at various stages of learning in supporting distinct sequence representations.

Key Words: Sequence representation, Anterior striatum, Posterior striatum, DLPFC, pre-SMA, SMA.

INTRODUCTION

It is commonly observed that when a skill is being acquired subjects are circumspect and deliberate in the initial attentive phase but later on as the skill is acquired they move into an automatic phase when attention can be engaged in other tasks simultaneously (Fitts, 1964). When performing well-mastered skills, it appears as if the body parts know what to do and no overt attention is necessary. Further, the memory of over-learned skills seems robust and lasts for long time. In this scenario it is interesting to find out if the representation of skill memory and the associated neural bases are different at various stages of learning. Previous studies on sequence learning addressed *where* and *when* activity is found in various cortical and subcortical areas using implicit learning (Grafton et al., 1995) and explicit learning by trial and error (Sakai et al., 1998; Toni et al., 1998). This paper addresses the question of *what* is actually learned in different areas at different stages of explicit sequence learning.

Earlier studies that investigated representational changes during motor sequence learning emphasized either implicit sequence learning in the serial reaction time (SRT) paradigm (Grafton et al., 1998), explicit sequencing but without learning (Harrington et al., 2000), or the recall of motor sequences at various stages of learning (Karni et al., 1995; Penhune and Doyon, 2002). Grafton et al. (1998) found learning-related increases in regional cerebral blood flow (rCBF) in the sensorimotor cortex reflecting effector-specific representation and in the inferior parietal cortex reflecting abstract representation of motor sequences. Sakai et al. (1998) and Toni et al. (1998) used trial and error learning paradigm to study the time course of changes during explicit visuo-motor sequence learning.

Hikosaka et al (2002) proposed that a sequence of movements is represented in two ways – spatial sequence and motor sequence. In their hypothetical scheme spatial sequence learning and representation are supported by parietal-prefrontal cortical loops with the associative region of the basal ganglia (anterior striatum) and cerebellum (posterior cerebellum). Motor sequence learning and representation are mediated by the motor cortical loops with the motor region of the basal ganglia (posterior striatum) and cerebellum (anterior cerebellum). Further, in their scheme premotor area mediates the transformation of spatial to motor coordinates and pre-supplementary motor area (pre-SMA) participates in coordination or switching between the two representations. In this connection it is interesting to note that this scheme is partly based on an earlier proposal of Alexander, DeLong, & Strick (1986) of distinct cortico-basal ganglia-thalamus loops serving different functions. In this scheme that stresses parallel information processing, the dorsolateral prefrontal cortex (DLPFC)–caudate nucleus loop takes part in spatial sequencing whereas the supplementary motor area (SMA)–putamen loop mediates motor sequencing.

Our hypothesis was that motor sequence learning involves two representations – an early acquisition of effector independent (abstract) representation and a late consolidation of effector dependent representation (Hikosaka et al., 1999, 2002; Bapi, Doya, & Harner, 2000; Nakahra, Doya, & Hikosaka, 2001). In an earlier behavioral study (Bapi et al., 2000), we used a sequential button-pressing task in which subjects performed either the same visuo-spatial sequence with altered finger movements or a different visuo-spatial sequence with the same finger movements. We found that the response time was significantly shorter when the finger movements remained the same compared to when the visuo-spatial sequence was the same. These results suggest that an effector independent representation develops early in the learning process and subsequently an effector dependent sequence representation is formed.

Using a whole-brain fMRI study, we set out to investigate the question of the brain areas subserving such representations acquired at various stages of explicit learning of motor sequences. In the current study, subjects learned a sequence of 12 finger movements, using a 2x6 task (Fig. 1 a) modified from Hikosaka et al. (1995), in two settings – *normal* setting where the visual display and keypad are arranged in the usual position and a *rotated* setting. In the *rotated* (*motor* and *visual*) conditions, subjects were required to rotate the visual cues by 180° and press the corresponding keys. The display sequence was also rotated for the *motor* condition, requiring an identical set of effector movements to be performed as in the *normal* condition. Thus the display-to-keypad mapping was identical for both the *motor* and *visual* settings. Further in the *visual* setting, the sequence remained the same as in *normal* in visuo-spatial coordinates, whereas it was different from *normal* in somato-motor coordinates. On the other hand, in the *motor* setting, the sequence in somato-motor coordinates was the same as in *normal*, but it was different from *normal* in visuo-spatial coordinates. This experimental design allowed us to explicitly tap into the neural loci of abstract and effector-specific representations of motor sequences.

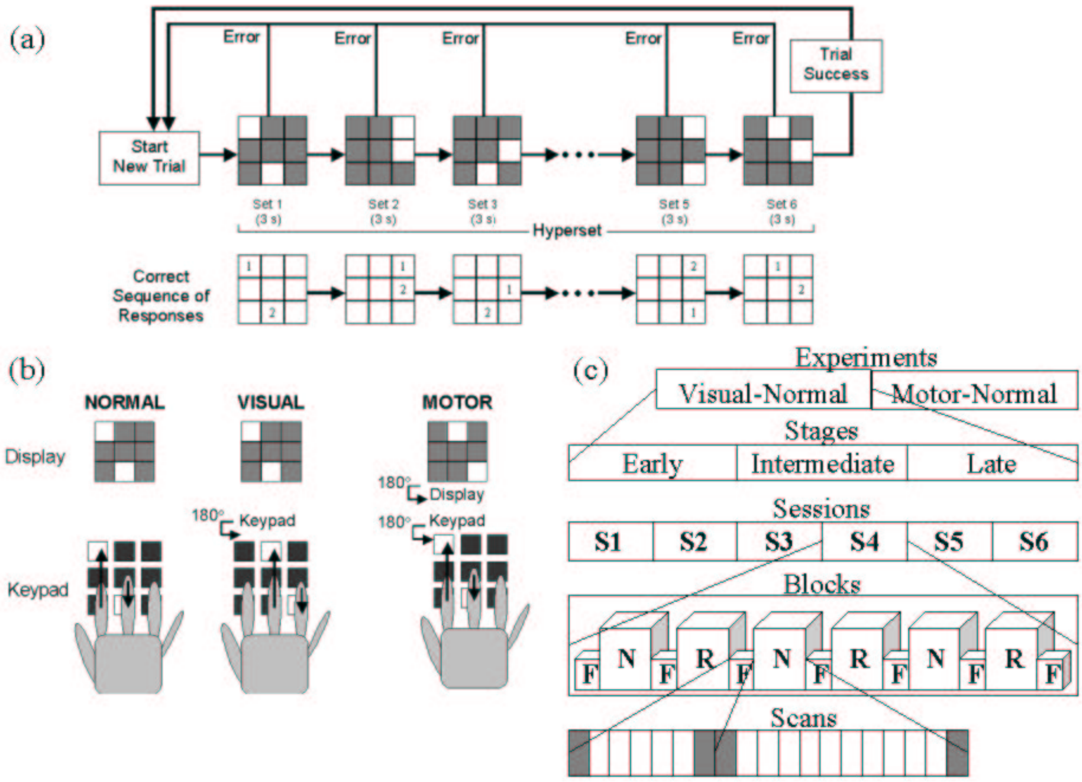

Figure 1. Sequence task setup. (a) In 2x6 sequence task, a sequence of 12 key presses is learned by trial and error, two at a time (called a ‘set’) in a series of six sets (called a ‘hyperset’). The two key presses belonging to a set need to be executed within 3 sec and after an appropriate delay the subsequent set is displayed. A new trial is started by resetting the presentation of the hyperset to the beginning either upon an error in any set or on successful completion of the entire hyperset. The bottom panel indicates the correct order of key presses for the example shown in the top panel. (b) *Normal* and *Rotated* settings for set 1 of the example are shown. In the *normal* setting the visual display and keypad are arranged in the usual upright position and in the *rotated* settings the display-to-keypad relationship was altered. In the *visual* setting, the keypad was *rotated* by 180°, while the display remained unaltered. In the *motor* setting both the keypad and the display on the screen were *rotated* by 180°. Consequently, in the *visual* setting the sequence of visuo-spatial cues (visuo-spatial sequence) remained identical, while in the *motor* setting the sequence of finger movements (somato-motor sequence) remained the same as that of the *normal* setting. Finger movements to be executed for an example are indicated by arrows in all the settings in the lower panel. Six such sets constituted a hyperset as shown in panel *a*. (c) Subjects performed two experiments – visual-normal and motor-normal. Each experiment consisted of six sessions of which the first two and the last two represented ' early' and ' late' stages of learning, respectively. We utilized an on-off (box-car) design for the experiments. In every session, subjects alternated between sequence learning tasks in the test blocks (N: *normal* and R: *rotated*) and followed random visual cues in the control blocks (F: *follow*). The duration of the test block was 36 sec and that of control block was 21 sec. 12 and 7 scans were acquired during the test and control blocks, respectively. Scans identified in gray shade represent instruction scans at the beginning and end of a block.

MATERIALS AND METHODS

Subjects

Ten normal (five female) right-handed subjects (ages 22 – 29 years) gave informed consent and were paid for their participation in the study. The experimental protocol was approved by the Ethics committee of the Laboratory for fMRI, Robarts Research Institute, London, Canada. Each subject contributed to two measurements by repeating the experiments on a different day. Subjects learned different sequences in the two repetitions of the experiments. Due to technical problems in data recording and large head movement, final data analysis was carried out on two repetitions by six subjects and one repetition by two other subjects.

Experimental task

We used a modified 2x6 sequence task (Hikosaka et al., 1995; Bapi et al., 2000). Two square cells (called a set) were illuminated simultaneously on the 3x3 grid. Subjects learned, by trial and error, the correct order of pressing the corresponding keys. A sequence of six such sets constitutes a hyperset. (Fig. 1 a). Subjects were asked to execute the sequence as fast as they could at all times to facilitate smooth performance of finger movements. We fixed the inter-set gap within a hyperset to 3 seconds to enable presentation of the sets at an even pace. Trial was terminated upon an error and learning started again from the beginning of the hyperset.

Normal and Rotated settings

Subjects practiced the same hyperset alternately in *normal* and *rotated* (*visual* or *motor*) settings (Fig. 1 b). While in the *normal* setting the display and keypad were arranged in the usual upright position, the display-to-keypad relationship was altered in the *rotated* settings. In the *visual* setting, the keypad was rotated by 180°, while the display remained unaltered. In the *motor* setting both the keypad and the display on the screen were rotated by 180°. Consequently, in the *visual* setting the sequence of visuo-spatial cues (visuo-spatial sequence) remained identical, while in the *motor* setting the sequence of finger movements (somato-motor sequence) remained the same as that of the *normal* setting. Further, it is to be noted that the display-to-keypad mapping was identical between the *motor* and *visual* settings.

Experiments

We utilized an on-off (box-car) design for the experiments where subjects alternated between control and test conditions (Fig. 1 c). In the control condition we used the 1x12 *follow* task wherein subjects pressed one key at a time following random visual cues. In the test condition we used the 2x6 sequence task and subjects practiced the same hyperset alternately in *normal* and *rotated* (*visual* or *motor*) settings. Before every scanning experiment, subjects performed the experimental tasks in a practice session for half-an-hour using a hyperset different from the one used during scanning. Subjects were informed of the display and keypad rotations and hence our task is an explicit sequence learning task.

Scan parameters

Scanning was done in a 4-Tesla Siemens/Varian MR whole-body imager at the laboratory for fMRI, Robarts Research Institute, University of Western Ontario, London, Canada. In each experiment, a time series of 726 whole-brain EPI images (interleaved Echo Planar pulse sequence) with an inter-scan interval of 3 seconds was acquired over a period of 6 sessions (Fig. 1c). Each scan consisted of 17 horizontal slices of 6 mm thickness [echo time (TE) 15 ms, 64x64 matrix size, 3.75 x 3.75 mm in-plane resolution, field of view (FOV) 24 cm]. In addition, a high-resolution anatomical image [Flash imaging sequence, TR 11 ms, TE 5.6 ms, 256x256 matrix size, 0.93 x 0.93 mm in-plane resolution] consisting of 64 slices separated by 3.3 mm, was collected for each subject.

Data Analysis

Behavioral analysis

While subjects performed experiments in the scanner, behavioral parameters reflecting the number of sets completed (accuracy) and the time taken to complete a set (response time) were measured for every block. Performance improvements within an experiment and across the *normal* and *rotated* settings were assessed using repeated-measures ANOVA. Based on the performance measures, we identified two learning periods – an early period comprising the first two sessions in an experiment where subjects were still slower and inaccurate and a late period comprising the last two sessions of an experiment where the subjects approached their maximal levels of performance.

Image analysis

The imaging data were analyzed using SPM99 (Wellcome Department of Cognitive Neurology, London). The functional images were reoriented to set the origin near the intersection of the coronal plane through AC and the AC-PC line and then motion correction was performed with respect to the first functional image in each session. Anatomical image for each subject was co-registered with the first functional image and then normalized to the T1 template from the International Consortium for Brain Mapping (ICBM) Project. The resulting parameters were used for normalizing all the functional images (Friston et al., 1995a) into Talairach stereotaxic space (Talairach and Tournoux, 1988). Spatial smoothing with a gaussian kernel of 8 mm FWHM was applied to the normalized images. The preprocessed data were analyzed using the general linear model framework (Friston et al., 1995b). For each subject, the experimental settings were modeled using boxcar functions convolved with the canonical hemodynamic response function in a session separable model. Data from all the six sessions was included. We report results from the early (first two sessions) and late stages (last two sessions) as the main focus of the experiment was to examine representational changes in sequence learning. Further, subject-specific variations in learning were taken into account by including the behavioral parameters (accuracy and response time) as user specified regressors. The regressors were constructed by giving a normalized score (range 0-100) reflecting improvements in learning for the sequence blocks. A score of 0 was assigned to the *follow* blocks as there was no learning involved.

Group analysis was performed using the random effects approach (Penny & Holmes, 2003) as implemented in the SPM99 software. Contrast images computed from the subject-specific models were entered into paired t-tests that accounted for the two repeated measures from the subjects. This model allowed for variance to be similar within subject and different across subjects. The voxel coordinates reported in the tables are transformed (Brett et al., 2001) from MNI to Talairach space. It was found that activated clusters spanned across several brain areas in the *rotated* > *follow* contrasts. For these contrasts, we counted the number of significant voxels using Talairach Daemon software (Lancaster et al. 2000). Location of peak activation for regions having more than 5 significant voxels were identified using ROI masks based on the the Talairach daemon with the help of WFU Pick Atlas software (Maldjian et al. 2003). For the other contrasts, the number of significant voxels per cluster has been reported.

Brain activation results at selected cortical and subcortical areas are overlaid on normalized structural MRI of one of the subjects' skull stripped using the Brain Extraction Tool (Smith, 2002) available in the MRIcro software (Rorden & Brett, 2000). Functional overlays on transverse slices were achieved using MRIcro software. At selected functional regions of interest, average blood oxygen-level dependent (BOLD) signal was calculated for each of the six sessions from a 3mm spherical volume for each subject. We performed brain-behavior correlation analysis taking average values across subjects (Bland & Altman, 1994). Pearson correlation coefficient (R) and its two-tailed significance level (p) were computed.

RESULTS

Behavioral Results

Two behavioral measures were calculated – the average number of sets completed per trial in a block indicating the accuracy (Fig. 2 a) and the average set completion time revealing the speed of performance (Fig. 2 b). Repeated measures ANOVA for the *follow* condition revealed that accuracy and response times were similar across the two experiments (visual-normal and motor-normal). Further there were no learning related improvements in the *follow* condition. Thus, *follow* serves as a stable baseline measure to assess the progress of performance in the test conditions.

Repeated measures ANOVA for the *normal* (*normalm, normalv*) and *rotated* (*motor, visual*) test conditions revealed significant ($p<0.0001$) improvements in accuracy and response times from the early to the late stage. Figure 2 shows comparisons between the test conditions across the two experiments. While the *normal* conditions had similar performance measures, the comparisons between the *rotated* settings revealed superior performance for the *motor* setting than the *visual* setting. While subjects attained accuracy levels similar to that of the *motor* setting by the late stage of *visual* setting, the response times remained significantly slower in both early and late stages of *visual* setting.

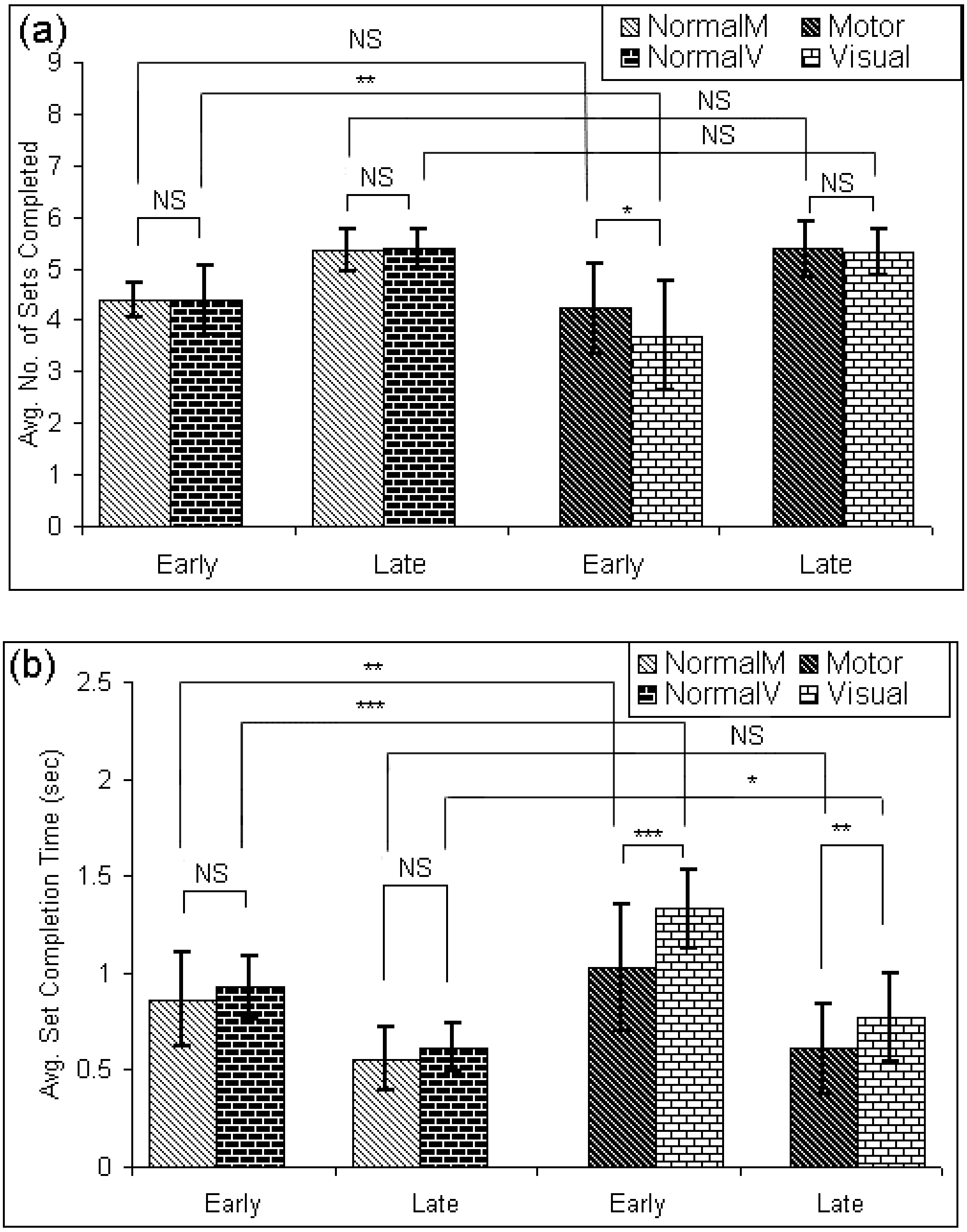

Figure 2. Behavioral results. a) Accuracy. Graph depicts the average number of sets completed (out of a maximum of 6 sets in a hyperset) in the early and late stages. As learning progressed, the number of sets completed (accuracy) increased significantly from early to late stage in all the settings ($p<0.0001$). Accuracy in the *normal* settings (*NormalM* and *NormalV*) was similar throughout the experiment. Although accuracy in the early stage seemed higher in the *motor* than in the *visual* setting, thereafter it remained similar in both the settings. b) Set completion time. Graph depicts the average set completion time (in sec) in the early and late stages. As learning progressed, it required significantly less time to perform a set. Again, while the completion times were similar in the *normal* settings (*NormalM* and *NormalV*), they were much shorter for the *motor* than for the *visual* setting. Significance levels: *** indicates $p<0.0001$, ** $p<0.001$ and * $p<0.01$, NS is Not Significant.

To investigate the underlying causes for slower response times in the *visual* setting, we performed correlation analysis of chunking patterns between the *normal* and *rotated* settings. It has been shown that subjects spontaneously reorganize the sequence into a number of chunks while learning the *mxn* task (Sakai et al. 2003, Pammi et al. 2004). We identified the chunking patterns using the response times for individual sets of the sequence. We assumed that the chunking patterns would have stabilized by the late stage. Figure 3 displays the average response times for the six sets in the late stage of *normal* and *rotated* settings for a representative subject. Since a trial was terminated upon error, only successful trials were used to calculate the chunking patterns. As shown in Figure 3, there was a significant correlation between the chunking patterns of the *normal* and *motor* settings, while the chunking patterns were different for the *normal* and *visual* settings. The correlation results for all the subjects are tabulated in the supplementary material. These results clearly indicate that subjects used similar representation of motor sequences for the *normal* and *motor* settings, but developed a different representation of the motor sequence in the *visual* setting. Taken together, high accuracy level and slower response times in the *visual* setting in the late stage suggest that subjects might have successfully acquired a second motor sequence in the *visual* setting.

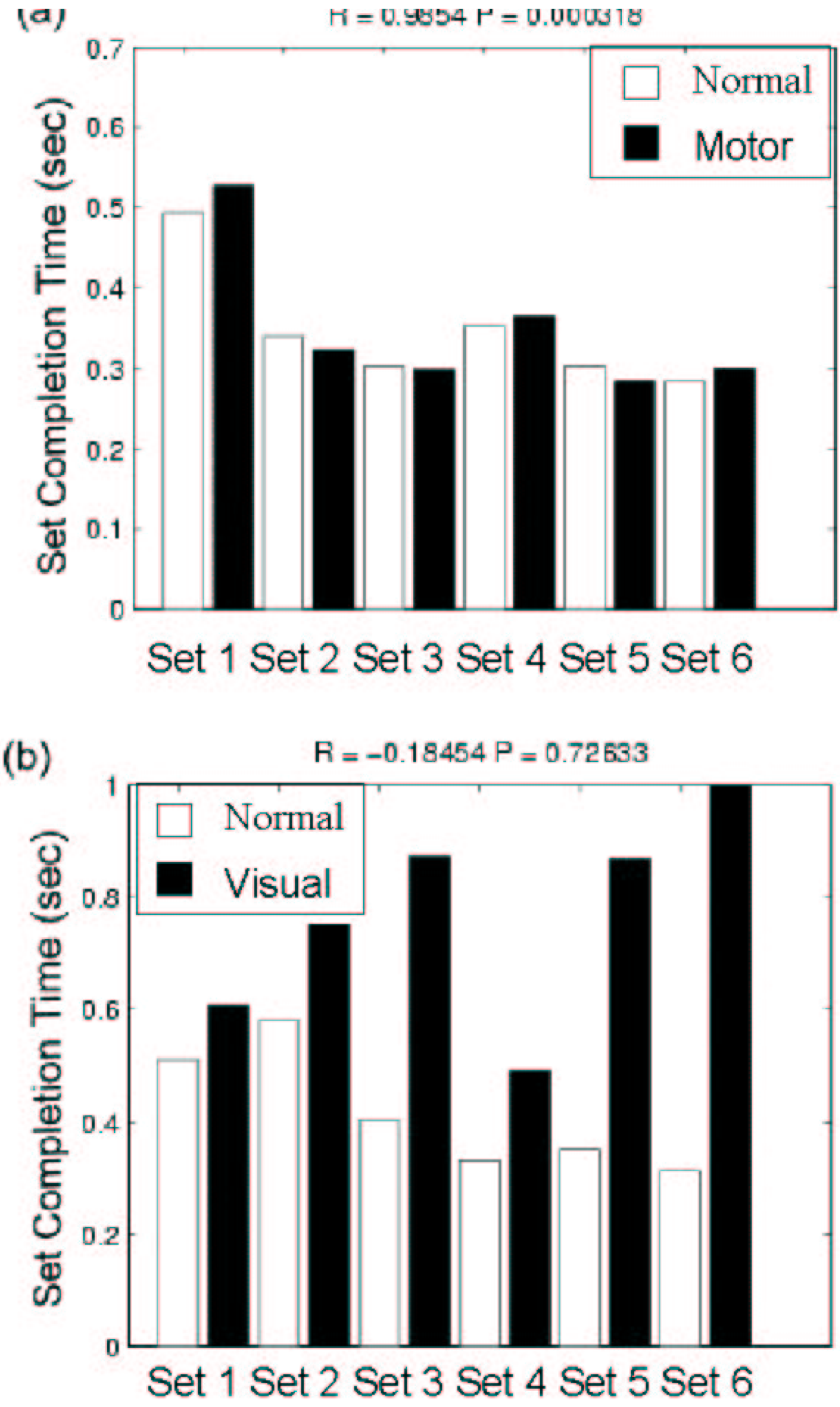

Figure 3. Chunking results. Response time profile in *motor* setting seems to coincide with that of *normalm* indicating a transfer of motor skill from the *normal* to the *motor* setting. In contrast the profile of RTs is distinctly different between *normalv* and *visual* settings pointing out that two motor sequence representations may have been acquired in the visual-normal experiments.

fMRI Results

Visual-normal experiments

All the activations associated with visual-normal experiments during both the early and late stages are summarized in Table 1 and Figure 4. In *visual* > *follow* contrast (Table 1a), sustained activation was found in the right cerebellum near the right superior vermis in the anterior lobe (culmen) in both early and late stages. Activations in other subcortical regions include the ventral striatum, caudate body, anterior and posterior regions of dorsal putamen, and right hippocampus. Activity in the left posterior putamen became stronger by the late stage. In addition, activation was also found in right middle temporal gyrus (BA 39) and extrastriate visual areas (BA 19). Activations in cortical regions include various regions of the parietal cortex, left primary motor cortex and dorsal premotor cortex. Activation in the pre-supplementary motor area (Pre-SMA) was observed in the late stage of *visual* setting. Activation in parietal regions was stronger in the left compared to the right hemisphere. The strength of activation in the left superior parietal cortex, left inferior parietal lobule (IPL) and left dorsal and ventral premotor areas showed an increasing trend from early to late stages. A transition of activation was observed from the parietal areas in the early stage to the parietal-premotor areas in the late stage of *visual* setting. In the *visual* > *normal* contrast (Table 1 b), activity was found in the early stage in the superior occipital gyrus as well as in the superior parietal cortex. In the late stage the activity was in the anterior putamen, inferior parietal cortex and medial frontal gyrus.

Table 1a. Locations of significant BOLD signal in the early and late stages of *visual* > *follow* contrast

			EARLY					LATE			
Brain area		voxels	Coordinates (mm)			*T* value	voxels	Coordinates (mm)			*T* value
			x	y	z			x	y	z	
Cerebellum (Culmen)	R	**105**	2	-49	-9	**4.13**	**111**	8	-66	-8	**6.5**
Thalamus (Pulvinar)	R	**73**	24	-29	3	**4.48***	**10**	20	-24	16	**3.34***
	L	**55**	-18	-23	14	**5.96***	**102**	-20	-31	9	**3.78**
Caudate Body	R	**80**	16	8	14	**5.19**	**13**	18	8	14	**4.17**
	L	**21**	-18	1	17	**6.94**	**77**	-20	-18	25	**6.52**
Anterior Putamen (dorsal)	R	**84**	24	8	12	**5.11***	**27**	20	3	15	**4.89**
	L	**167**	-24	4	3	**5.84**	**128**	-16	1	11	**5.54**
Posterior Putamen (dorsal)	R	**35**	22	-1	15	**5.75**	**58**	30	-2	2	**3.33***
	L	**160**	-30	-8	0	**6.63**	**275**	-28	-2	4	**8.08**
Globus Pallidus	R	**0**		----			**9**	22	-14	-1	**4.11***
	L	**52**	-16	0	9	**4.62**	**83**	-16	-1	9	**4.84***
Ventral Striatum	R	**0**		----			**53**	34	-20	-2	**4.85**
	L	**98**	-28	-6	-6	**4.38***	**68**	-28	-4	-5	**3.66***
Hippocampus	R	**6**	32	-33	-3	**3.13***	**21**	32	-29	-7	**4.08***
	L	**0**		----			**0**		---		
Middle Temporal Gyrus (BA 39)	R	**15**	42	-71	26	**4.54**	**25**	48	-67	13	**3.86**
	L	**2**		----			**0**		----		
Superior Occipital Gyrus (BA 19)	R	**16**	36	-74	28	**4.16**	**16**	38	-78	26	**5.8**

	L	**8**	-36	-78	32	**4.5***	**0**		----		
Middle Occipital Gyrus (BA 18/19)	R	**3**		----			**10**	28	-79	9	**3.67**
	L	**17**	-30	-79	19	**4.09**	**14**	-38	-72	7	**3.45**
Superior Parietal Cortex (BA 7)	R	**102**	32	-66	47	**6.37**	**61**	28	-46	58	**6.05**
	L	**172**	-24	-51	58	**6.72**	**117**	-24	-50	56	**7.46**
Inferior Parietal Lobule (BA 40)	R	**97**	42	-31	40	**3.98**	**95**	44	-33	48	**5.93**
	L	**357**	-40	-44	54	**6.81**	**242**	-36	-40	55	**9.8**
Precuneus (BA 7)	R	**104**	12	-55	58	**4.73**	**69**	10	-56	47	**3.98**
	L	**108**	-20	-56	53	**8.77***	**131**	-12	-57	54	**4.21***
Primary Motor Cortex (BA 4)	L	**15**	-40	-19	38	**4.69***	**22**	-30	-27	46	**4.98**
Sensory (BA 2/3)	L	**146**	-55	-27	44	**5.63**	**166**	-55	-25	44	**6.96**
Premotor (dorsal) (BA 6)	R	**0**		----			**7**	-40	0	39	**10.3**
	L	**40**	-32	-6	41	**4.68**	**46**	32	6	42	**6.41**
Premotor (ventral) (BA 6)	R	**0**		----			**0**		----		
	L	**9**	-36	0	35	**5.59***	**37**	-48	-3	26	**4.58**
Pre-SMA (BA 6)		**0**		----			**13**	-2	14	45	**3.8**

Stereotaxic Talairach coordinates of peak activation obtained with $p < .005$ (uncorrected). Coordinates of peak activation are reported for regions having atleast 5 significant voxels. * indicates that the peak was identified using a ROI mask as clusters of activations spanned across several brain regions.

Table 1b. Locations of significant BOLD signal in the early and late stages of *visual* > *normal* contrast

		EARLY					LATE				
Brain area		**Cluster size (voxels)**	Coordinates (mm)			***T* value**	**Cluster size (voxels)**	Coordinates (mm)			***T* value**
			x	y	z			x	y	z	
Anterior Putamen(d)	L			----			**21**	-26	2	7	**4.57**
Superior Occipital Gyrus (BA 19)	R	**21**	34	-76	28	**3.49**			----		
Superior Parietal Cortex (BA 7)	R	**43**	34	-58	51	**3.23**			----		
	L	**121**	-16	-57	58	**4.74**			----		
Inferior Parietal Cortex (BA 40)	L			----			**6**	-44	-37	31	**3.28**
Medial Frontal Gyrus (BA 9)				---			**9**	18	40	15	**3.34**

Stereotaxic Talairach coordinates of peak activation obtained with $p < .005$ (uncorrected).

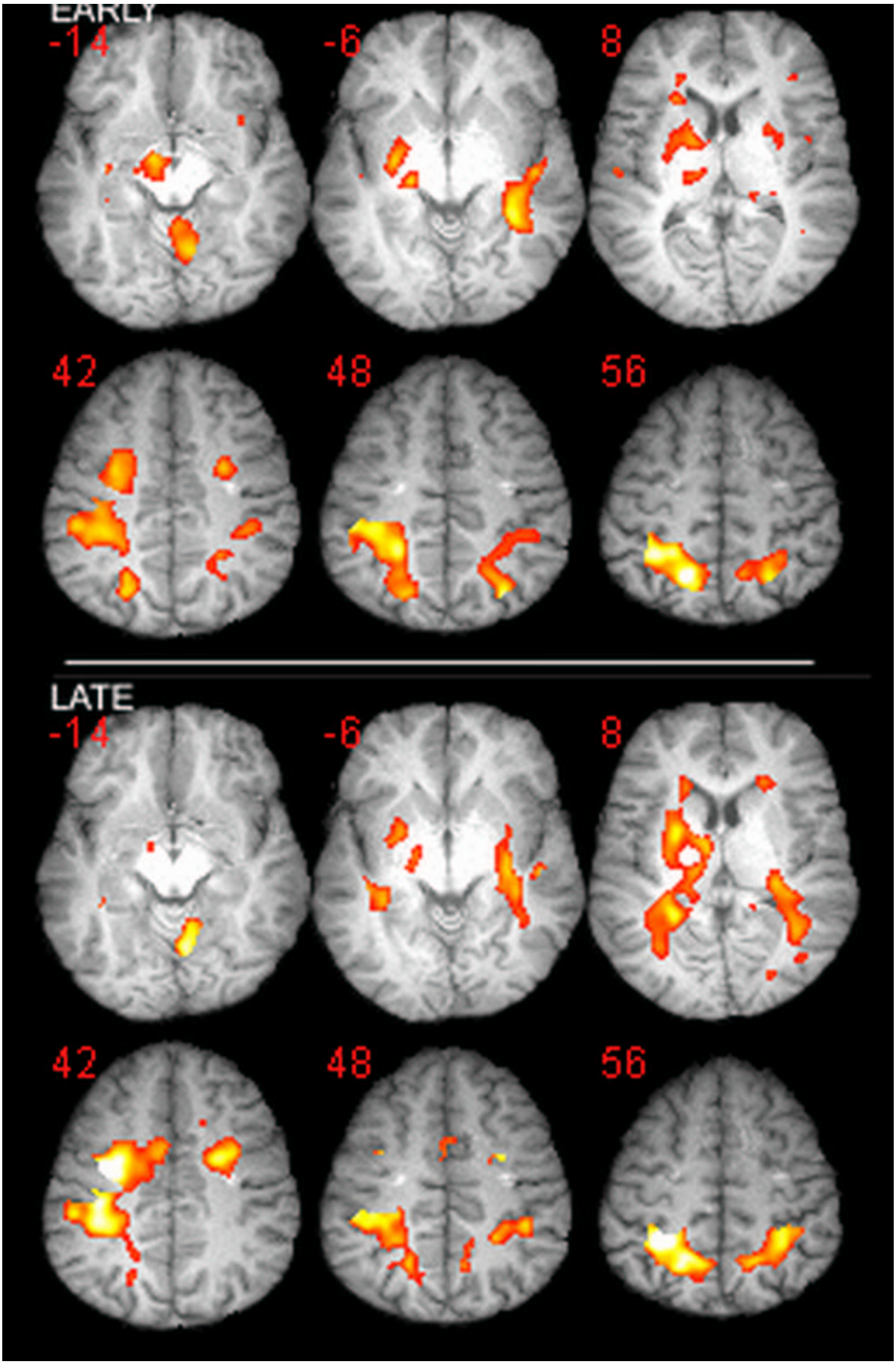

Figure 4. Brain activation in the *visual* setting. Slice overlays depicting some of the subcortical and cortical activations found in the *visual* setting compared to the *follow*. Color scale indicates T values of activation thresholded at $p<.005$ ranging from 0 to 7. Activations are overlaid on one of the subjects' skull-stripped normalized structural MRI. Top panel shows activations in early stage and bottom panel shows activations in late stage. The slices are selected to represent activations in the right anterior cerebellum (z=-14 mm), ventral striatum (z= -6 mm) and dorsal putamen(z=8 mm) in the top row and Inferior Parietal (z= 42), dorsal premotor cortex (z=42), Pre-SMA(z=48) and Superior Parietal cortex(z=56) in the bottom row.

Motor-normal experiments

All the activations associated with motor-normal experiments during both the early and late stages are summarized in Table 2 and Figure 5. In *motor* > *follow* contrast (Table 2a), there is a general trend of decrease in activation from early to late stage in various subcortical regions such as in the anterior lobe (culmen) of right cerebellum, bilateral thalamus (pulvinar), right caudate body, bilateral dorsal putamen (anterior and posterior aspects), and bilateral globus pallidus. However, the trend in the cortical regions is a mixed one. Sustained activity was found in the left inferior parietal lobule, left primary motor cortex, and left somatosensory cortex. While there is no residual activity in the right middle temporal gyrus and right middle occipital gyrus by the late stage, activity in the left middle occipital gyrus decreased by the late stage. Activation was found bilaterally in the superior parietal cortex, inferior parietal lobule and precuneus in both early and late stages. An increase in activation was observed in both the dorsal and ventral regions of left premotor. While the activation in superior parietal cortex seems to decrease from early to the late stage, that in the dorsal premotor area in the left hemisphere becomes stronger by the late stage of *motor* setting. Thus a transition of activation seems to be taking place from the parietal-premotor areas in the early stage to premotor areas by the late stage of *motor* setting. Interesting thing to note is the absence of activity in the anterior dorsal striatum by the late stage and lack of any activity in the ventral striatum and the hippocampus in the *motor* setting. In *motor* > *normal* contrast, persistent activity was found in the left superior and inferior parietal cortical areas and in the early stage an additional locus of activation was found in the right middle temporal gyrus (Table 2 b).

Table 2a. Locations of significant BOLD signal in the early and late stages of *motor* > *follow* contrast

		EARLY					LATE				
Brain area		**voxels**	Coordinates (mm)			***T* value**	**voxels**	Coordinates (mm)			***T* value**
			x	y	z			x	y	z	
Cerebellum (Culmen)	R	**130**	10	-65	-9	**5.88**	**26**	6	-65	-9	**4.2**
Thalamus (Pulvinar)	R	**49**	24	-29	5	**4.94***	**0**		----		
	L	**53**	-4	-31	9	**4.66**	**2**		----		
Caudate Body	R	**30**	10	5	13	**3.55**	**7**	14	6	7	**4.6**
	L	**3**		----			**12**	-16	16	14	**3.81**
Ant. Putamen (dorsal)	R	**44**	26	8	11	**4.48**	**3**		----		
	L	**10**	-24	3	13	**2.89***	**1**		----		
Post. Putamen (dorsal)	R	**193**	32	-9	6	**3.86**	**5**	24	-5	19	**4.16**
	L	**178**	-22	-3	15	**5.05**	**45**	-28	-4	6	**3.62**
Globus Pallidus	R	**27**	22	-6	4	**4.14**	**1**		----		
	L	**39**	-20	-11	4	**4.38***	**0**		----		
Middle Temporal Gyrus (BA 39)	R	**10**	42	-69	15	**4.44**	**0**		----		
	L	**1**		----			**0**		----		
Superior Occipital Gyrus (BA 19)	R	**1**		----			**0**		----		
	L	**5**	-36	-78	32	**3.84***	**0**		----		
Middle Occipital Gyrus (BA 18/19)	R	**16**	28	-79	17	**4.13**	**0**		----		
	L	**28**	-28	-77	17	**5.35**	**16**	-26	-85	19	**4.11**
Superior Parietal Cortex (BA 7)	R	**65**	18	-47	61	**4.05**	**47**	24	-50	58	**5.85**

	L	**76**	-20	-49	60	**7.5**	**98**	-24	-56	53	**5.89**
Inferior Parietal Lobule (BA 40)	R	**44**	32	-38	50	**3.52**	**23**	36	-31	35	**3.99**
	L	**262**	-44	-36	52	**4.28**	**289**	-48	-33	40	**6.21**
Precuneus (BA 7)	R	**79**	20	-52	54	**4.92***	**9**	20	-52	56	**4.28***
	L	**126**	-20	-56	53	**8.34***	**64**	-20	-54	54	**4.98***
Primary Motor Cortex (BA 4)	L	**13**	-51	-16	34	**4.01**	**17**	-59	-19	40	**4.27**
Sensory (BA 2/3)	L	**143**	-44	-29	51	**4.31**	**169**	-48	-26	31	**6.71**
Premotor (dorsal) (BA 6)	R	**4**		----			**12**	28	4	40	**7.47**
	L	**18**	-30	-2	41	**4.78**	**45**	-32	4	40	**7.81**
Premotor (ventral) (BA 6)	R	**2**		----			**0**		----		
	L	**13**	-53	2	31	**2.98**	**63**	-42	-1	28	**5.45**
Middle Frontal Gyrus (BA 9/46)	R	**14**	44	8	35	**3.82**	**0**		----		
	L	**0**		----			**26**	-48	6	35	**5.73**

Stereotaxic Talairach coordinates of peak activation obtained with $p < .005$ (uncorrected). Coordinates of peak activation are reported for regions having atleast 5 significant voxels. * indicates that the peak was identified using a ROI mask as clusters of activations spanned across several brain regions.

Table 2b. Locations of significant BOLD signal in the early and late stages of *motor* > *normal* contrast

		EARLY					LATE				
Brain area		**Cluster size (voxels)**	Coordinates (mm)			***T* value**	**Cluster size (voxels)**	**Coordinates (mm)**			***T* value**
			x	y	z			x	y	z	
Middle Temporal Gyrus (BA 39)	R	**7**	51	-63	25	**3.24**			---		
Superior Parietal Cortex (BA 7)	L	**15**	-21	-61	55	**3.19**	**10**	-34	-54	51	**3.8**
Inferior Parietal Lobule (BA 40)	L	**7+4**	-36	-42	46	**3.3**	**23**	-46	-37	39	**3.63**

Stereotaxic Talairach coordinates of peak activation obtained with $p < .005$ (uncorrected).

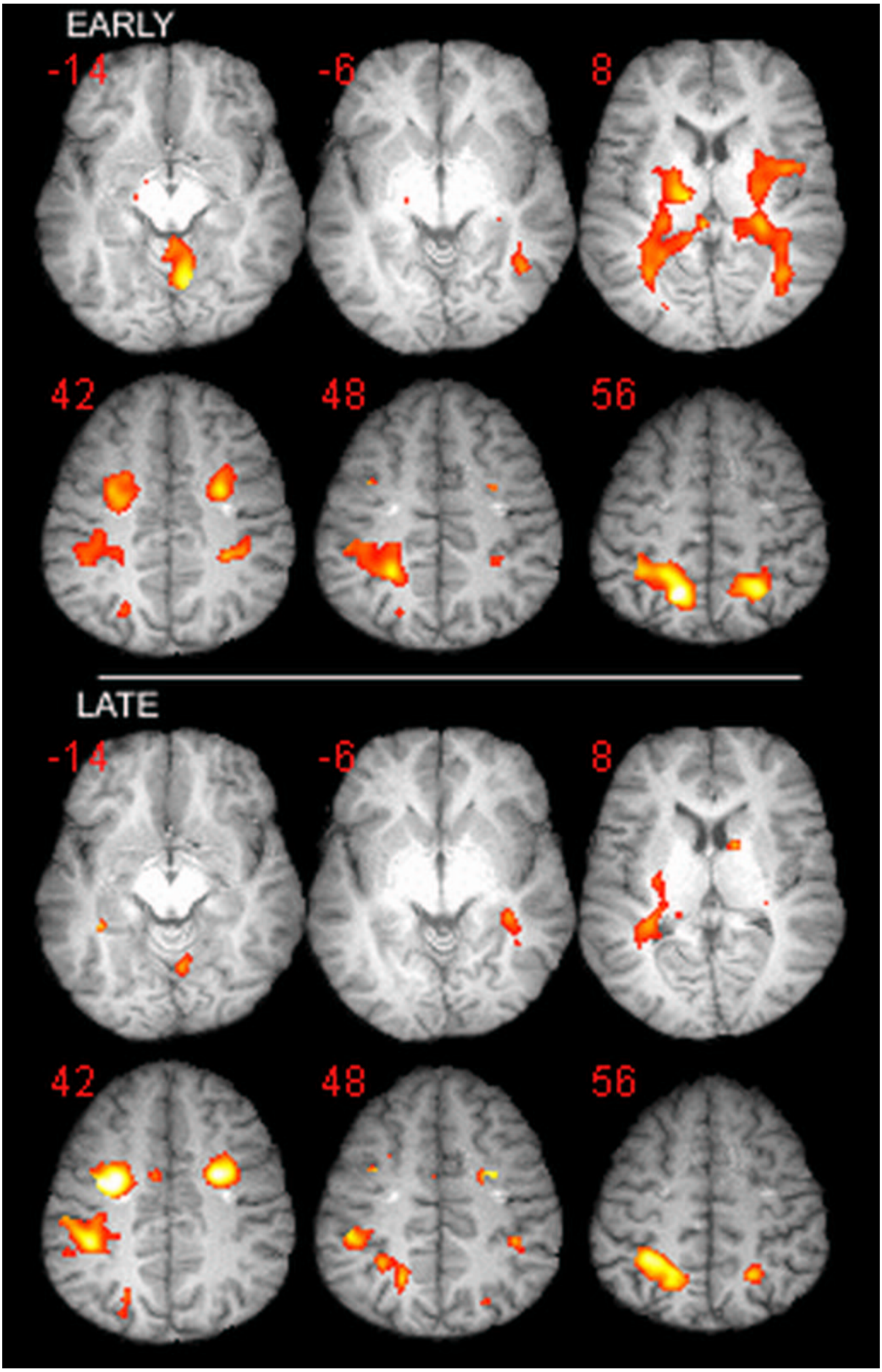

Figure 5. Brain activation in the *motor* setting. Slice overlays depicting some of the subcortical and cortical activations observed in the *motor* setting compared to the *follow*. See Figure 4 legend for further description.

Distinct neural systems subserving sequence representations

Direct comparison of visual and motor contrasts would reveal distinct neural systems associated with the *visual* and *motor* settings, respectively (Table 3). In the early *visual* > *motor* comparison, left anterior putamen in the dorsal aspect, left ventral striatum and left hippocampus were activated. Apart from the subcortical activity, activation of the medial prefrontal cortex, anterior cingulate, right superior parietal cortex, and right occipital cortex near the middle occipital gyrus were also observed. Similarly, extensive cortical and subcortical activation was also observed in the late stage. Subcortical activation loci were found in the left dorsal putamen (anterior region) and left hippocampus. The activation in the left dorsal putamen was stronger in the late stage and extended into posterior putamen also. Cortical activation was in the precuneus, middle frontal gyrus, the occipital lobe, and the temporal lobe (BA 39). An interesting observation is the transition of activity observed from the left anterior putamen to left anterior and posterior putamen by the late stage in the *visual* setting (Table 3).

While the *visual* setting activated several subcortical and cortical sites, activity in the *motor* setting was restricted mainly to cortical loci. In the early *motor* > *visual* contrast, activation was observed in the precuneus, right occipital cortex near the lingual, fusiform and middle occipital gyri and in the right inferior frontal gyrus (IFG). While activation in the right IFG remained till the late stage, additional areas in the left prefrontal cortex (BA 9, 10 and 45), anterior cingulate, and caudal supplementary motor area (SMA) were activated in the late stage. There were activations in the right cerebellum (anterior lobe) and left caudate body in the late stage of the *motor* setting.

Table 3. Locations of significant BOLD signal comparing the two *rotated* conditions

Brain area		**Cluster size (voxels)**	Coordinates (mm)			***T* value**
			x	y	z	
Early v*isual* > *motor*						
Ventral Striatum	L	**3+3**	-32	-12	-8	**2.93**
Anterior Putamen (dorsal)	L	**3**	-26	4	2	**2.96**
Hippocampus	L	**11**	-30	-22	-11	**3.27**
Brodmann Area 19	R	**23**	36	-41	-3	**3.47**
	L	**5**	-26	-68	-3	**2.94**
Medial Frontal Gyrus (BA 9) +		**155**	-4	38	29	**3.85**
Anterior Cingulate (BA 32)			-6	30	22	**3.47**
Late v*isual* > *motor*						
Caudate Body	L	**19+24**	-18	-18	23	**3.59**
Medial Globus Pallidus	L	**6**	-18	-14	-4	**3.06**
Hippocampus	L	**3**	-28	-35	0	**3.04**
Anterior Putamen (dorsal)	L	**95**	-30	4	3	**4.08**
Thalamus (Pulvinar)	L	**4**	-14	-23	7	**2.98**

Middle Occipital Gyrus (BA 19)	R	**158**	22	-89	8	**4.66**
Inferior Parietal Lobule (BA 40)	L	**21**	-28	-38	53	**3.33**
Superior Parietal Cortex (BA 7)	R	**6**	14	-55	58	**3.12**
Precuneus (BA 7)	R	**41**	8	-54	47	**3.71**
Middle Frontal Gyrus (BA 10)	R	**10**	34	38	18	**3.69**
Early *motor* > v*isual*						
Brodmann Area 19	R	**42**	28	-81	17	**3.97**
Brodmann Area 18	R	**15**	30	-78	-3	**3.56**
	L	**11**	-6	-69	15	**3.43**
Cingulate Gyrus (BA 31)	R	**96**	16	-53	28	**3.7**
	L	**9**	-16	-45	28	**3.02**
Precuneus (BA 7)	L	**165**	-16	-70	37	**4.53**
Inferior Frontal Gyrus (BA 45)	R	**3**	55	20	5	**3.12**
Late *motor* > v*isual*						
Anterior Cerebellum (Culmen)	R	**9**	12	-34	-10	**3.07**
Caudate Body	L	**3**	-8	5	16	**3.17**
Anterior Cingulate (BA 32)	L	**6**	-6	41	7	**3.06**
SMA (BA 6)		**7**	0	-25	53	**3.22**
Superior Frontal Gyrus (BA 10)	R	**4**	-28	48	23	**3.18**
Middle Frontal Gyrus (BA 9)	L	**11**	-44	11	33	**3.53**
Inferior Frontal Gyrus (BA 45)	R	**3**	57	26	15	**3.15**
	L	**12**	-53	22	8	**3.37**
Medial Frontal Gyrus		**5**	-8	53	16	**3.46**

Stereotaxic Talairach coordinates of peak activation obtained with $p < .005$ (uncorrected).

Summary of main effects and direct comparisons

While activation in the right anterior cerebellum sustained from the early to late stage of *visual* setting, the activity decreased by the late stage in the *motor* setting. Whereas the activation in the left dorsal putamen extended into both anterior and posterior regions in the *visual* setting, that in the *motor* setting was found to be concentrated within the posterior region. Further, activation in the putamen became stronger from early to late stage in the *visual* setting, but it decreased by the late stage in *motor* setting. Activation in the ventral striatum and hippocampus was found only in the *visual* setting. There seems to be a trend of shift in activation from the parietal in early *visual* to parietal-premotor areas in late *visual* and early *motor* settings. The activation in premotor areas became stronger by the late stage of *motor* setting. The pre-SMA was active only in the late stage of *visual* setting and the caudal SMA only in the late stage of *motor* setting.

Brain-behavior correlation (BBC) analysis

In Table 4 we report the results from regression analysis of brain activation with the two behavioral parameters. Areas that have a positive correlation in *visual* setting would reflect sequence learning related changes while those with the *motor* setting would be related to performance of the somato-motor sequence. Correlation results depicted in Figures 6 and 7 clearly establish the role for pre-SMA in the *visual* setting and that for the SMA in the *motor* setting. Correlation results indicate that as performance improved in both the *rotated* settings, the activity in the right DLPFC and the right superior parietal cortex decreased possibly reflecting processes related to motor sequence learning and performance (Jenkins et al., 1994; Jueptner et al., 1997a&b; Grafton, Hazeltine, & Ivry, 1998). As performance improved in the *visual* setting, activity in pre-SMA, left ventral premotor increased and that in the left hippocampus decreased. On the other hand as performance became over-learned in the *motor* setting, activity in SMA and left dorsal premotor increased and that in the left inferior parietal cortex and precuneus decreased.

Table 4. Brain behaviour correlations in the *rotated* settings

					VISUAL				***MOTOR***			
Brain area		Coordinates (mm)			***Correlation (Accuracy)***		***Correlation (Response Time)***		***Correlation (Accuracy)***		***Correlation (Response Time)***	
		x	y	Z	R	P	R	P	R	P	R	P
Ant. Cerebellum (Culmen)	R	10	-65	-9	+0.80	0.058	-0.76	0.08	+0.34	0.51	-0.37	0.47
Hippocampus	L	-22	-35	-10	-0.96	< 0.01	+0.96	< 0.01	+0.25	0.63	-0.22	0.68
Ant. Putamen (d)	L	-26	6	5	+0.78	0.067	-0.74	0.94	+0.077	0.89	-0.087	0.87
Post Putamen (d)	L	-26	-9	10	+0.81	< 0.05	-0.78	0.06	+0.13	0.81	-0.11	0.84
Post. Putamen (d)	L	-26	-2	0	+0.41	0.41	-0.41	0.42	+0.77	0.07	-0.77	0.07
Sup. Parietal Cortex (BA 7)	R	34	-58	51	-0.85	< 0.05	+0.89	< 0.05	-0.82	< 0.05	+0.81	0.052
Inf. Parietal Lobe (BA 40)	L	-34	-54	40	-0.65	0.16	+0.72	0.11	-0.85	< 0.05	+0.87	< 0.05
Precuneus (BA 7)	R	4	-58	51	-0.29	0.58	+0.36	0.48	-0.94	< 0.01	+0.93	< 0.01
	L	-6	-63	51	-0.49	0.32	+0.57	0.23	-0.88	< 0.05	+0.87	< 0.05
Premotor (dorsal) (BA 6)	L	-40	-2	41	+0.37	0.47	-0.33	0.52	+0.81	< 0.05	-0.85	< 0.05
Premotor (ventral) (BA 6)	L	-55	1	26	+0.98	< 0.001	-0.97	<0.001	-0.08	0.87	+0.14	0.79
Pre-SMA (BA 6)		-4	8	46	+0.99	< 0.0001	-0.99	< 0.0001	+0.39	0.44	-0.38	0.46
SMA (BA 6)		-6	-17	49	+0.18	0.73	-0.16	0.75	+0.87	< 0.05	-0.86	< 0.05
Middle Frontal Gyrus (BA 46)	R	30	19	34	-0.81	0.051	+0.84	< 0.05	-0.84	< 0.05	+0.84	< 0.05

Correlation of Brain activation with behavioural measures. Abbreviations: Sup. Superior, d Dorsal, Ant. Anterior, Post. Posterior

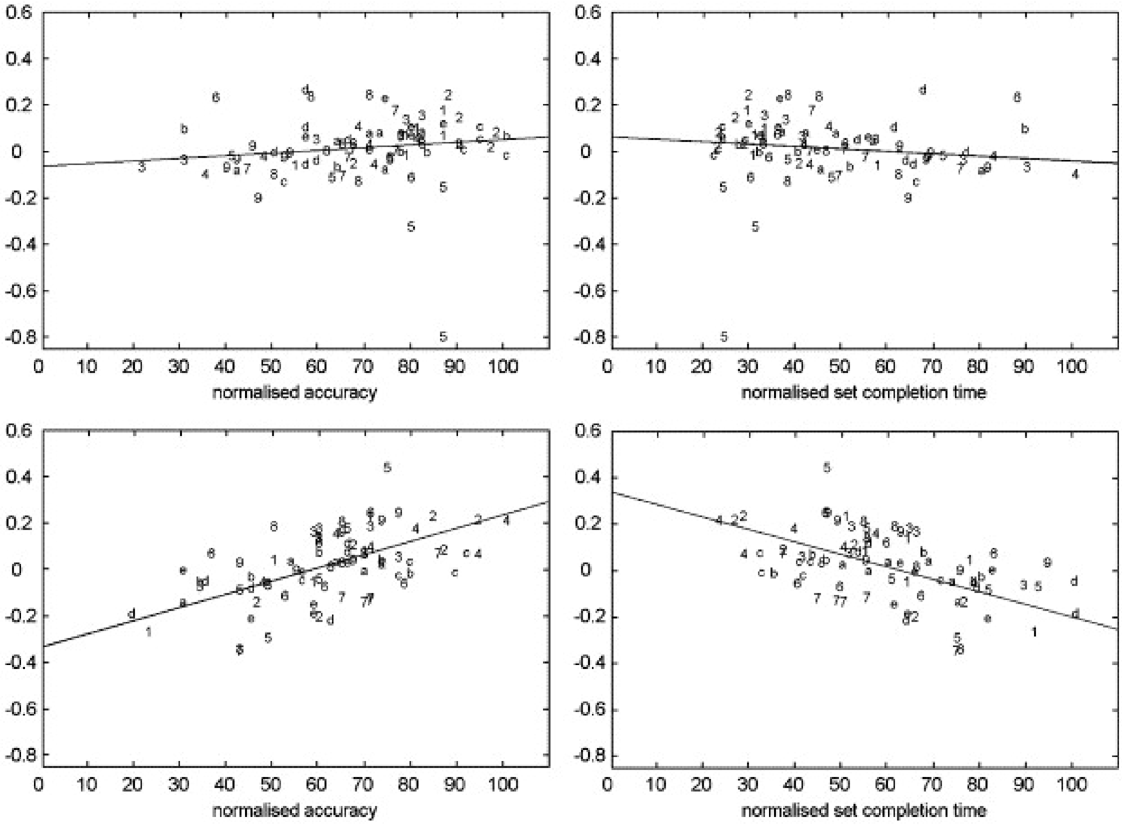

Figure 6. Brain-behavior correlation at Pre-SMA. Voxel data were extracted from a 3 mm spherical VOI defined at Pre-SMA (Talairach coordinates x=-4, y=8, z=46 mm; Table 3b) and the average BOLD signal for each of the six sessions was calculated for each subject separately for *motor* and *visual* experiments. Average performance measures were calculated for the six sessions for each subject separately for the two experiments. Graph depicts the scatter plot between the normalized behavioral measure (accuracy: left panel and set completion time: right panel) and the BOLD signal for each subject (1 – 9 and a – e). The regression line fits the average values of behavioral measure and the BOLD signal. The top panel shows the results for *motor* setting and the bottom panel for the *visual* setting. The correlation results are: *Motor* [Accuracy: R = 0.39, *p*=0.44; Time: R = -0.38, *p*=0.46]; *Visual* [Accuracy: R = 0.99, *p*<.0001; Time: R = -0.99, *p*<.0001]. Clearly, the activity in pre-SMA is closely related to performance improvements in the *visual* setting but not the *motor* setting.

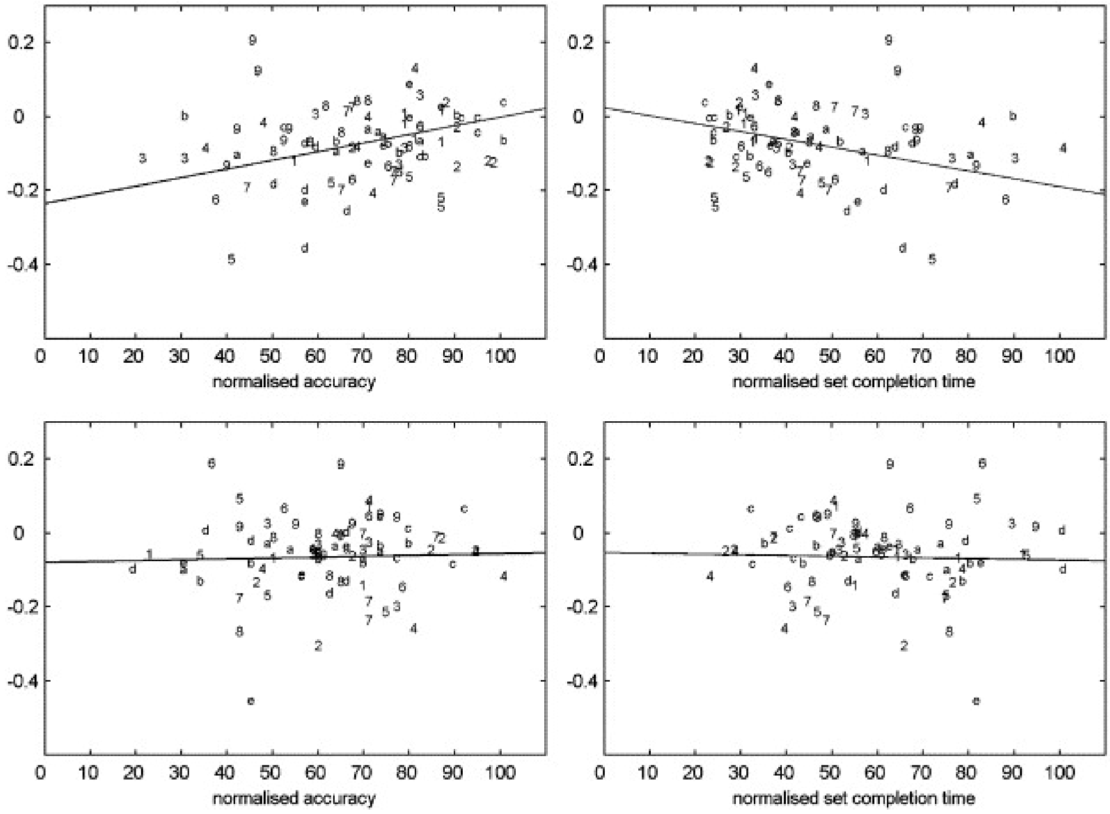

Figure 7. Brain-behavior correlation at SMA. The correlation analysis procedure is described in the caption for Figure 6. Voxel data were extracted from a VOI defined at SMA (Talairach coordinates x=-6, y=-17, z=49 mm; Table 4a). The top panel shows the results for *motor* setting and the bottom panel for the *visual* setting. The correlation results are: *Motor* [Accuracy: R = 0.87, $p<.05$; Time: R = -0.86, $p<.05$]; *Visual* [Accuracy: R = 0.18, $p=0.73$; Time: R = -0.16, $p=0.75$]. Clearly, the activity in SMA is closely related to performance improvements in the *motor* setting but not the *visual* setting.

Discussion

The aim of the study was to investigate different representations of visuomotor sequences as learning progressed from the early to the late stage. We demonstrated that response times were shorter when subjects used effector-specific information (as in the *motor* setting) than when they utilized abstract sequential information based on visual cues (in the *visual* setting). We identified the subcortical and cortical brain areas that mediated the two sequence representations. Firstly, left anterior putamen in the dorsal striatum was found to be selectively active in the *visual* setting. Secondly, it appears that when sequences are learned utilizing visuo-spatial representation, the focus of activation moved from parietal in the early stage to parietal-premotor areas in the late stage. In contrast, when sequences were performed with an emphasis on the somato-motor representation, the transition was in the opposite direction, that is, from parietal-premotor in the early to premotor areas in the late stage.

It is known that visuo-spatial sequence representation can be acquired quite quickly but somato-motor optimization takes time (Bapi et al., 2000; Nakahara et al., 2001). In the *visual* setting, although subjects attained similar level of accuracy to that of *motor* setting by the late stage, performance speed was significantly slower (Fig. 2). Behavioral results further indicated that the subjects utilized abstract sequential information provided by the visual cues over an extended period of time and eventually learned a new somato-motor sequence in the *visual* setting. Superior performance speed in the *motor* setting by the early stage itself (Fig. 2) underlines the advantage of using effector-specific representation. We further demonstrated that chunking patterns of the sequences were identical between the *motor* and *normal* settings (Fig. 3). Thus, while the onset of learning of visuo-spatial and somato-motor sequence representations is the same, the activity associated with each setting at various stages pointed out how learning of the representations unfolded over time. The unique experimental design we used in this study enabled us to tap into the representations that facilitate the learning of motor sequences and their unfolding process.

Subcortical structures

While activation in the right anterior cerebellum sustained from the early to late stage of *visual* setting (Table 1a), the activity decreased by the late stage in the *motor* setting (Table 2a). Anterior cerebellum might possibly be involved in the optimization of movement parameter and timing information in both the sequence representations (Jueptner & Weiller, 1998; Sakai et al., 2000). Based on previous studies involving trial and error learning (Jenkins et al., 1994; Jueptner et al., 1997b), sustained activity observed in the ventral striatum in both early and late stages of *visual* setting may be attributed to the trial and error process adopted for cue selection. Interestingly, when there was no emphasis on cue selection process as in the *motor* setting, ventral striatal activity was absent. Further evidence comes from the activation of ventral striatum observed in the *direct* comparison contrast of early *visual* > *motor* (Table 3). Left putamen activation in the dorsal striatum extended into both anterior and posterior regions in the *visual* setting (Table 1a), whereas in the *motor* setting activation was found exclusively within the posterior putamen (Table 2a). Further, left anterior putamen in the dorsal striatum was found to be selectively active in the *visual* setting (Table 3). Additionally, while activation in the putamen became stronger from the early to late stage in the *visual* setting, it decreased by the late stage in the *motor* setting (Table 1a, 2a). Another structure that can possibly be implicated with visuo-spatial representation is the hippocampus, which was found to be activated in early and late stages of *visual* > *motor* contrast (Table 3). The brain behaviour relationship in the hippocampus was significantly correlated with the *visual* setting, but not the *motor* setting (Table 4). In contrast to earlier studies where cerebellum (Doyon et al. 2003) and basal ganglia (Penhune & Doyon, 2002; Shadmehr & Holcomb, 1997) activity was not observed during the recall stage, the activity in these regions persisted till the more automatic late stage in the *motor* setting. One possible reason for this is that in our experiment, recall was measured within the experimental session on the same day as opposed to the earlier studies where recall was assessed after a delayed consolidation period. The conclusions on cerebellum are provisional as the coverage of cerebellum did not extend into posterior lobe in the fMRI scans at the chosen field of view.

Cortical structures

There seems to be a trend of shift in activation from the parietal in early *visual* to parietal-premotor areas in late *visual* (Table 1a) and early *motor* settings (Table 2a). The activation in premotor areas becomes stronger by the late stage of *motor* setting (Table 2a). The trend of shift in parietal areas is strengthened by its activation in the late *visual* > *motor* comparison and early *motor* > *visual* contrasts (Table 3). The brain behaviour relationships clearly demonstrate a decreasing trend of activation in the parietal areas and an increasing trend of activation in the premotor areas for the *motor* setting (Table 4). The activation in the frontal areas did not show any selectivity to either of the rotated settings (Table 3 and 4). The rostral part of supplementary motor area, pre-SMA, was selectively active in the late stage of *visual* setting (Table 2a). In the visual-normal experiments subjects used the same visuo-spatial sequence but learned two motor sequences, one corresponding to the *normal* and the other to the *visual* setting. The brain-behavioral relationship result of pre-SMA (Fig. 6, Table 4) combined with the selective activation found in the late but not in the early stage of *visual* setting (see Table 1a) indicates its role in new somato-motor sequence learning process. The activation of pre-SMA during new motor sequence learning was also observed in earlier studies (Hikosaka et al., 1996; Sakai et al., 1998). Together with the activity observed in the anterior cingulate (Table 3), we speculate that the pre-SMA may have a dual role, one in sequence learning and the other in sequence switching (Shima et al., 1996). Consistent with the explicit and implicit sequence learning literature (Tanji & Shima, 1994; Grafton, Hazeltine, & Ivry, 1998; Willingham, 1998; Keele et al., 2003; Tanji, 2001), we found SMA activity in the late stage of *motor* setting (Table 3) and brain- behaviour correlation (Fig. 7, Table 4) reflecting its role in somato-motor sequence representation. We observed activity in M1 during somato-motor sequence learning and performance as evidenced by its activation in early and late stages of both the *rotated* settings. These results suggest that M1 participates in the learning of motor sequences but may not be the actual locus of representation. These observations on M1 are consistent with most of the earlier proposals for its role in motor learning (for example Karni et al., 1995; Grafton et al., 1998; Sanes, 2003). We can speculate that activity in the right DLPFC observed in both the *rotated* settings (decreasing trend as seen in Table 4) is related to the optimization of the sequencing process.

It is possible that the *rotated* > *normal* contrasts point out learning related activations in addition to rotational transformations. Our experimental design involved interleaved blocks of *normal* and *rotated* settings alternating with the *follow* condition. Both the *normal* and *rotated* settings involved sequence learning, whereas the *follow* condition did not involve any learning. Hence, we associate any activity observed in the subtractions reflected in *rotated* > *normal* contrasts with rotational transformations, but not with sequence learning. Activity observed in the superior occipital gyrus and superior parietal cortex in the *visual* > *normal* contrast (Table 1b) may support processes involved in target rotation and the activity in the middle temporal gyrus and inferior parietal cortex in the *motor* > *normal* contrast (Table 2b) may be related to the processes involved in cue rotation.

Brain areas supporting the formation of representations during sequence learning

Our results suggest that visuo-spatial sequence representation engages cortical and subcortical network involving the left anterior striatum, hippocampus, extrastriate visual areas, dorsal and ventral premotor, and parietal cortical areas (see Table 1a, 3). The activation in the extrastriate visual areas may be related to the visuo-motor processes required for synchronizing the motor actions to visual cues (Bower, 1995). The activation in the extrastriate visual areas and hippocampus may form part of the ventral stream (Mishkin, Ungerleider, & Macko, 1983) that encodes information in visual coordinates and conveys the information to ventral premotor to enable the formation of visual stimulus-to-response associations (Caminiti, Ferraina, & Mayer, 1998). The activity in the parietal cortex may be part of the dorsal stream (Mishkin, Ungerleider, & Macko, 1983) conveying information in spatial coordinates to the dorsal premotor to enable formation of spatial cue-to-response associations (Wise et al., 1997). Anterior striatum may be in the best position to combine the information from the ventral and dorsal streams to formulate goal-directed action sequences based on abstract information. Our results also revealed that effector-specific sequence representation is subserved by the dorsal premotor and SMA (Table 3, 4). A summary of our findings on various representations acquired during the process of visuomotor sequence learning is given in the supplementary figure (Fig. S4).

Cortico-subcortical networks subserving visuo-spatial and somato-motor sequence representations

Our hypothesis in sequence learning is that the early stage involves *abstract* (*visuo-spatial*) representation and the late stage involves effector-specific (*somato-motor*) representation. This is true regardless of whether subjects are performing the sequence task in the *normal*, *motor* or *visual* settings in our experiments or they are learning some other visuo-motor skill such as cycling or boxing. The usual acquisition of visuo-spatial sequence being very rapid, we designed the visual-normal experiment so that subjects were required to use the sequence of visual cues over an extended period and eventually acquired a second motor sequence for the *visual* setting. The design strategy of the motor-normal experiments was such that subjects could focus on motor movement sequence right from the early stage and progress to performance of an over-learned somato-motor sequence. Ours is an explicit sequence learning task and the instructions and pretraining given to the subjects ensured that subjects took advantage of the representations that were being learned at various stages of the task (see Experiments subsection in Materials and Methods). However, it is possible that there are alternative explanations for the results we obtained.

First, subjects might simply be performing the display and keypad rotations to retrieve the sequence from the *normal* setting in order to perform the *rotated* settings. This is not likely given that the accuracy was similar for the *motor* and *normal* settings in both early and late stages. The *visual* setting had accuracy similar to *normal* by late stage (Fig. 2). Further if subjects had continued to use rotational transformations till the late stage, we would not observe improvements in response times from the early to the late stage.

Second, subjects might develop novel representations for the sequence in *rotated* settings independently from the sequence in the *normal* setting. This is not likely given that subjects are slower in the *visual* setting compared to the *motor* setting in both the early and late stages. We have manipulated the display and keypad rotations such that display-to-keypad mapping is the same in *visual* and *motor* settings. If subjects did not benefit from the sequence in the *normal* setting, then improvements in performance must be similar for the two *rotated* settings and that is clearly not the case (Fig. 2).

Third, it is possible that in both the *rotated* settings, subjects simply learned to apply rotational transformations in the initial phase to learn the correct sequence but eventually learned to replace this difficult operation with a novel sequence representation. We suggest that this is a more plausible explanation for sequence learning tasks that require performing a rotational transformation such as the current experiment. Given that the visuo-spatial representation is acquired fairly quickly during sequence learning (for example, in the *normal* setting), the *visual* setting stretches this representation over a longer period of time as evidenced by its slower performance indices. Similarly, given that a somato-motor representation takes quite long to establish, the *motor* setting extends this late stage of sequence learning into the early stage of the *motor* setting by using strategies of explicit sequence learning. Thus the tasks appear to bias the sequence learning process in the two experiments the way we intended.

The shift in activity from anterior putamen in early *visual* (Table 1a, 3) to posterior putamen in late *visual* (Table 1a) and early *motor* settings and finally to the posterior putamen in the late stage of *motor* setting (Table 2a) seems to have a cortical analog. The transition of activity from the parietal cortex in the early *visual* setting to conjoint activity in the pariteal-premotor areas in the late *visual* as well as early *motor* and subsequently to the dominant activity in the premotor cortex in the late stage of *motor* setting seems to mirror the type of transitions taking place in the basal ganglia regions. Anterior striatum is part of the prefrontal and parietal cortex – basal ganglia loops which may be involved in the visuo-spatial representation whereas posterior striatum as part of the primary and secondary motor cortex – basal ganglia loops may be involved in the somato-motor sequence representation (Alexander, DeLong, & Strick, 1986; Hikosaka et al., 2002).

The novelty of our current findings is that the differential involvement of the cortico-subcortical loops subserving various sequence representations could be demonstrated as a direct outcome of our experimental design. The results suggest that during the process of learning, an early acquisition of visuo-spatial representation is subserved by frontal, parietal cortex – anterior striatal loop followed by an additional recruitment of secondary motor areas (dorsal premotor cortex and SMA) – posterior striatal loop during the acquisition of somato-motor representation. Finally, these results form the first comprehensive and direct evidence for the model proposed by Nakahara, Doya,

& Hikosaka (2001). The current results additionally suggest that possible reason for activation of different cortical and subcortical networks at various stages of sequence learning is to support two kinds of representation — abstract (visuo-spatial) in the early stage and effector-specific (somato-motor) in the late stage.

References

Alexander, G.E., DeLong, M.R., Strick, P.L., 1986. Parallel organization of functionally segregated circuits linking basal ganglia and cortex. *Ann. Rev. Neurosci. 9*, 357–381.

Bapi, R.S., Doya, K., Harner, A.M., 2000. Evidence for effector independent and effector dependent representations and their differential time course of acquisition during motor sequence learning. *Exp. Brain Res. 132*, 149–162.

Bland, J.M., Altman, D.G., 1994. Correlation, regression, and repeated data. *BMJ 308*, 896.

Bower, J., 1995. The cerebellum as a sensory acquisition controller. *Hum. Brain Mapp.* 2, 255–256.

Brett, M., Christoff, K., Cusack, R., Lancaster, J., 2001. Using the Talairach atlas with the MNI template. *NeuroImage, 13*, S85.

Caminiti, R., Ferraina, S., Mayer, A.B., 1998. Visuomotor transformations: Early cortical mechanisms of reaching. *Curr. Opin. Neurobiol. 8*, 753–761.

Doyon, J., Penhune, V., Ungerleider, L.G., 2003. Distinct contribution of the cortico-striatal and cortico-cerebellar systems to motor skill learning. *Neuropsychologia 41(3)*, 252–262.

Fitts, P.M., (1964). Perceptual-motor skill learning. In A.W. Melton (ed), *Categories of human learning*. Academic Press, New York, pp 243--285.

Friston, K.J., Ashburner, J., Frith, C.D., Poline, J-B., Heather, J.D., Frackowiak, R.S. J., 1995a. Spatial registration and normalisation of images. *Hum. Brain Mapp. 2*, 165-189.

Friston, K.J., Holmes, A.P., Worsley, K.J., Poline, J-B., Frith, C.D., Frackowiak, R.S. J., 1995b. Statistical parametric maps in functional imaging: A general linear approach. *Hum. Brain Mapp. 2*, 189–210.

Grafton, S.T., Hazeltine, E., Ivry, R., 1995. Functional mapping of sequence learning in normal humans. *J. Cog. Neurosci. 7*, 497–510.

Grafton, S.T., Hazeltine, E., Ivry, R.B., 1998. Abstract and effector-specific representations of motor sequences identified with PET. *J. Neurosci. 18*, 9420–9428.

Harrington, D.L., Rao, S.M., Haaland, K.Y., Bobholz, J.A., Mayer, A.R., Binder, J.R., Cox, R.W., 2000. Specialized neural systems underlying representations of sequential movements. *J. Cog. Neurosci. 12*, 56-77.

Hikosaka, O., Rand, M.K., Miyachi, S., Miyashita, K., 1995. Learning of sequential movements in the monkey: Process of learning and retention of memory. *J. Neurophysiol. 74*, 1652–1661.

Hikosaka, O., Sakai, K., Miyauchi, S., Takino, R., Sasaki, Y., Putz, B., 1996. Activation of human presupplementary motor area in learning of sequential procedures: a functional MRI study. *J. Neurophysiol. 76*, 617–621.

Hikosaka, O., Nakahara, H., Rand, M.K., Sakai, K., Lu, X., Nakamura, K., Miyachi, S., Doya, K., 1999. Parallel neural networks for learning sequential procedures. *Trends Neurosci. 22*, 464–471.

Hikosaka, O., Nakamura, K., Sakai, K., & Nakahara, H., 2002. Central mechanisms of motor skill learning. *Curr. Opin. Neurobiol. 12*, 217–222.

Holmes, A.P., Friston, K.J., 1998. Generalisability, random effects and population inference. *NeuroImage 7,* S754.

Jenkins, I.H., Brooks, D.J., Nixon, P.D., Frackowiak, R.S., Passingham, R.E., 1994. Motor sequence learning: A study with positron emission tomography. *J. Neurosci. 14*, 3775–3790.

Jueptner, M., Stephan, K.M., Frith, C.D., Brooks, D.J., Frackowiak, R.S.J., Passingham, R.E., 1997a. Anatomy of motor learning. I. Frontal cortex and attention to action. *J. Neurophysiol. 77,* 1313–1324.

Jueptner, M., Frith, C.D., Brooks, D.J., Frackowiak, R.S.J., Passingham, R.E., 1997b. Anatomy of motor learning. II. Subcortical structures and learning by trial and error. *J. Neurophysiol. 77*, 1325–1337.

Jueptner, M., Weiller, C., 1998. A review of differences between basal ganglia and cerebellar control of movements as revealed by functional imaging studies. *Brain 121*, 1437–1449.

Karni, A., Meyer, G., Jezzard, P., Adams, M.M., Turner, R., Ungerleider, L.G., 1995. Functional MRI evidence for adult motor cortex plasticity during motor skill learning. *Nature 377,* 155–158.

Keele, S.W., Ivry, R., Mayr, U., Hazeltine, E., 2003. The cognitive and neural architecture of sequence representation. *Psychol. Rev. 110(2)*, 316–339.

Lancaster, J.L., Woldorff, M.G., Parsons, L.M., Liotti, M., Freitas, C.S., Rainey, L., Kochunov, P.V., Nickerson, D., Mikiten, S.A., Fox, P.T., 2000. Automated Talairach atlas labels for functional brain mapping. *Hum. Brain Mapp. 10*, 120–131.

Maldjian, J.A., Laurienti, P.J., Kraft, R.A., Burdette, J.H., 2003. An automated method for neuroanatomic and cytoarchitectonic atlas-based interrogation of fmri data sets. *NeuroImage 19*, 1233–1239.

Mishkin, M., Ungerleider, L.G., Macko, K.A., 1983. Object vision and spatial vision: Two cortical pathways. *Trends Neurosci. 6*, 414–417.

Nakahara, H., Doya, K., Hikosaka, O., 2001. Parallel cortico basal ganglia mechanisms for acquisition and execution of visuomotor sequences – a computational approach. *J. Cog Neurosci. 13*, 626–647.

Pammi, V. S. C., Miyapuram, K. P., Bapi, R. S., & Doya, K., 2004. Chunking Phenomenon in Complex Sequential Skill Learning in Humans. In Pal, N.R., Kasabov, N., Mudi, R.K., Pal, S., Parui, S.K. (Eds.), *Lecture Notes in Computer Science,* Springer-Verlag Heidelberg, *3316*, 294– 299.

Penhune, V.B., Doyon, J., 2002. Dynamic cortical and subcortical networks in learning and delayed recall of timed motor sequences. *J. Neurosci. 22(4)*, 1397–1406.

Penny, W.D., Holmes, A.P., Friston, K.J., 2003. Random effects analysis. In R.S.J. Frackowiak, K.J. Friston, C. Frith, R. Dolan, K.J. Friston, C.J. Price, S. Zeki, J. Ashburner, and W.D. Penny (ed), *Human Brain Function*. Academic Press, 2nd edition.

Rorden C, Brett M., 2000. Stereotaxic display of brain lesions. *Behav Neurology 12(4)*, 191–200.

Sakai, K., Hikosaka, O., Miyauchi, S., Takino, R., Sasaki, Y., Putz, B., 1998. Transition of brain activation from frontal to parietal areas in visuomotor sequence learning. *J. Neurosci. 18*, 1827–1840.

Sakai, K., Hikosaka, O., Takino, R., Miyauchi, S., Nielsen, M., Tamada, T., 2000. What and when–parallel and convergent processing in motor control. *J. Neurosci. 20*, 2691–2700.

Sakai, K., Kitaguchi, K., & Hikosaka, O., 2003. Chunking during human visuomotor sequence learning. *Exp. Brain Res.*, *132*, 149–162.

Sanes, J.N., 2003. Neocortical mechanisms in motor learning. *Curr. Opin. Neurobiol. 13*, 225–231.

Shadmehr, R., Holcomb, H.H., 1997. Neural Correlates of *Motor* Memory Consolidation, *Science*, *277*, 821-825.

Shima, K., Mushiake, H., Saito, N., Tanji, J., 1996. Role for cells in the presupplementary motor area in updating motor plans. *Proc. Nat. Acad. Sci.*, *USA 93(16)*, 8694–8698.

Smith, S.M., 2002. Fast robust automated brain extraction. *Hum. Brain Mapp. 17(3)*, 143–155.

Talairach, J., Tournoux, P., 1988. *Co-planar stereotaxic atlas of the human brain*. New York: Thieme.

Tanji, J., Shima, K., 1994. Role of supplementary motor areas cells in planning several movements ahead. *Nature 371*, 413–416.

Tanji, J., 2001. Sequential organization of multiple movements: Involvement of cortical motor areas. *Ann. Rev. Neurosci. 24*, 631–651.

Toni, I., Krams, M., Turner, R., Passingham, R.E., 1998. The time course of changes during motor sequence learning: a whole-brain fMRI study. *NeuroImage 8*, 50–61.

Willingham, D.B., 1998. A neuropsychological theory of motor skill learning. *Psychol. Rev. 105*, 558–584.

Wise, S.P., Boussaoud, D., Johnson, P.B., Caminiti, R., 1997. Premotor and parietal cortex: Corticocortical connectivity and combinatorial computations. *Ann. Rev. Neurosci. 20*, 25–42.

Supplementary Material

Subjects: Ten subjects participated in the two experiments – Visual-Normal and Motor-Normal. Each subject participated twice, thereby contributing two measurements on two different days. Out of these, data from six pairs of experiments was not included in the analysis due to technical problems in data recording (2 pairs of data) and large head movement parameters identified in the realignment process (4 pairs of data). Our analysis is based on a total of 14 pairs of data (six subjects participating in two repetitions and two subjects contributing one measurement each).

Experimental Task.

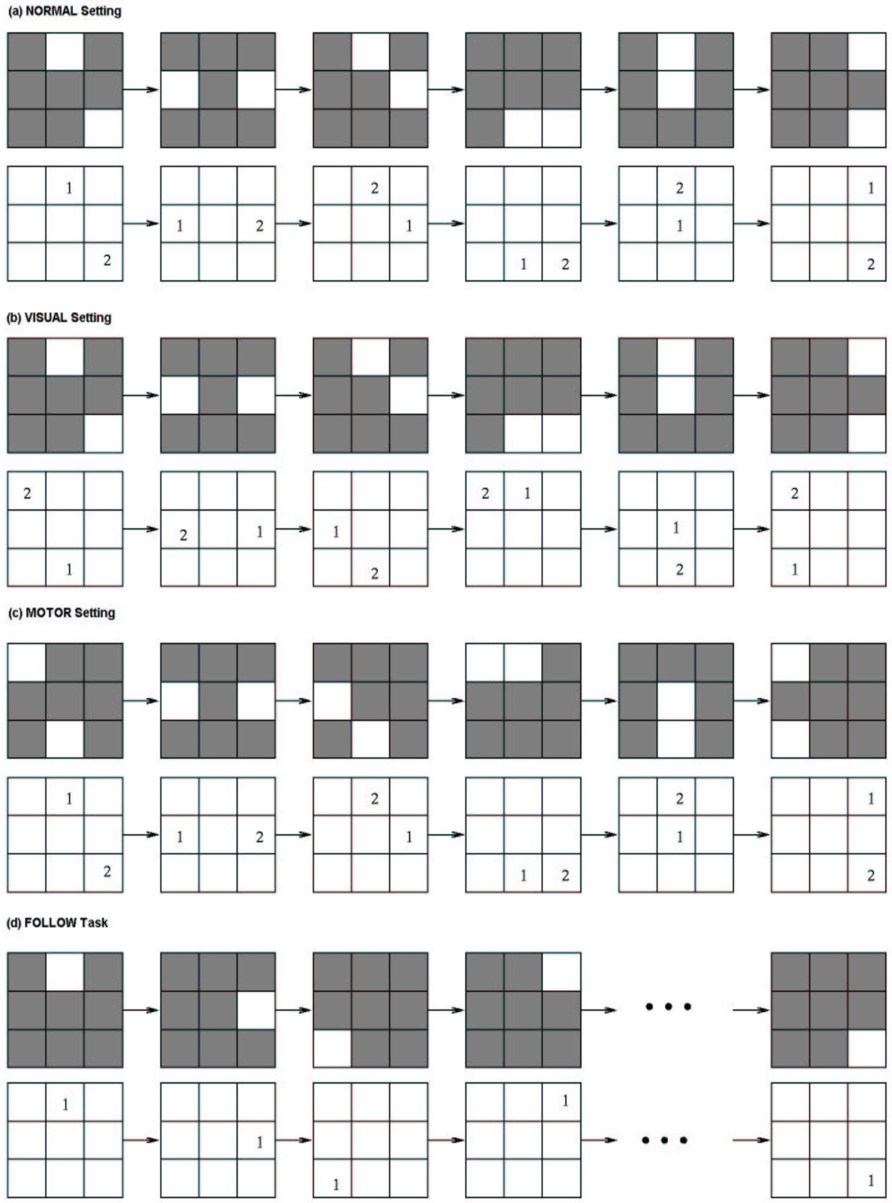

Figure S1: Subjects performed 2x6 sequence tasks in either (a) *Normal*, (b) *Visual* or (c) *Motor* settings. For each task, the top panel shows the visual display and the bottom panel indicates the correct order of responses on the keypad. Display and Keypad rotations for both the *visual* and *motor* settings is shown for the example sequence of *normal* setting shown in panel *a*. The baseline was random hypersets arranged as 1x12 sequences in the (d) *follow* condition. Subjects repeatedly practised the same hyperset for the sequence tasks *a* – *c*, but random hypersets were generated for every trial of the *follow* condition.

Behavioral Results.

Figure S2: Vertical lines in A and B demarcate the early, intermediate and late stages each consisting of 6 blocks. A) Accuracy. Graph depicts the average number of sets completed (out of a maximum of 6 sets in a hyperset) per block, averaged across subjects. As learning progressed, the number of sets completed (accuracy) increased significantly from early to late stage in all the settings. Accuracy in the *normal* settings (*NormalM* and *NormalV*) was similar throughout the experiment. Although accuracy in the early stage seemed higher in the *motor* than in the *visual* setting, thereafter it remained similar in both the settings. B) Set completion time. Graph depicts the average set completion time (in sec) per block, averaged across subjects. As learning progressed, it required significantly less time to perform a set. Again, while the completion times were similar in the *normal* settings (*NormalM* and *NormalV*), they were much shorter for the *motor* than for the *visual* setting.

Results from Repeated Measures ANOVA analysis for the Accuracy and Set completion times are tabulated in Table S1. To investigate the slower performance in *visual* setting as compared to the *motor* setting, we performed additional analysis of set completion times in the late stage. We tested for the correlation between the sequence structures of the *rotated* and corresponding *normal* settings. For this, we averaged set completion times for each of the six sets for successfully completed hypersets in the late stage of each experiment. The correlations reported in Table S2 clearly point out the similarity of the motor sequence structure used by the subjects between the *motor* and *normalm* settings (11 out of 14 measurements). In contrast, a lack of correlation was observed between the *visual* and *normalv* settings (13 out of 14 measurements). This result points out that the sequence structures acquired in the *visual* and *normalv* settings are different.

Table S1a: Main Effects of Repeated Measures ANOVA

	Accuracy		**Response Time**	
Sequence Tasks				
Setting	$F_{(3,39)} = 2.81$	$p = 0.052$	$F_{(3,39)} = 21.798$	$p < 0.0001$
Stage	$F_{(2,26)} = 98.88$	$p < 0.0001$	$F_{(2,26)} = 52.948$	$p < 0.0001$
Setting x Stage	$F_{(6,78)} = 1.408$	$p = 0.22$	$F_{(6,78)} = 3.88$	$p < 0.005$
Follow Task				
Experiment	$F_{(1,13)} = 0.829$	$p =0.379$	$F_{(1,13)} = 0.02$	$p = 0.89$
Stage	$F_{(2,26)} = 0.899$	$p = 0.419$	$F_{(2,26)} = 2.64$	$p = 0.09$
Experiment x Stage	$F_{(2,26)} = 1.082$	$p = 0.353$	$F_{(2,26)} = 0.671$	$p = 0.52$

Setting (4): NormalM, Motor, NormalV, Visual
Stage (3): Early, Intermediate, Late
Experiment (2): Motor-Normal, Visual-Normal

Table S1b: Post-hoc means comparison for Sequence Tasks

	Accuracy		**Response Time**	
Early Vs Late	F(1,78)	p	F(1,78)	p
NormalM	25.20	<< 0.0001	43.46	<< 0.0001
Motor	35.36	<< 0.0001	82.50	<< 0.0001
NormalV	25.94	<< 0.0001	44.99	<< 0.0001
Visual	68.29	<< 0.0001	143.40	<< 0.0001

Table S1c: Post-hoc means comparison for Sequence Tasks

	Accuracy				**Response Time**			
	Early		Late		Early		Late	
	F(1,78)	P	F(1,78)	p	F(1,78)	p	F(1,78)	p
Nm Vs M	0.60	0.44	0.02	0.88	12.82	< 0.001	1.19	0.28
Nv Vs V	13.00	< 0.001	0.19	0.66	74.46	<< 0.0001	11.30	< 0.005
M Vs V	7.53	< 0.01	0.18	0.67	41.05	<< 0.0001	12.36	< 0.001
Nm Vs Nv	0.01	0.93	0.03	0.87	1.84	0.18	1.55	0.22

Nm: NormalM, M: Motor, Nv:NormalV, V: Visual

Table S2: Correlation of set completion Times

	Motor and NormalM		Visual and NormalV	
Subject	R	P	R	P
BG1	0.99	0.0002	0.84	0.0366
CB1	0.96	0.0028	0.33	0.5238
CT1	0.99	0.0003	-0.18	0.7263
KN1	0.97	0.0015	0.02	0.9643
LF1	0.99	0.0001	0.76	0.0765
RB1	0.87	0.0238	0.45	0.3654
BG2	0.97	0.0015	0.01	0.9862
CB2	-0.12	0.8268	0.69	0.1323
CT2	0.96	0.0028	0.45	0.3651
KN2	-0.12	0.8203	0.17	0.7450
KZ2	0.85	0.0306	-0.65	0.1622
LF2	0.98	0.0004	0.54	0.2712
LA2	0.91	0.0123	-0.21	0.6899
RB2	0.81	0.0503	0.69	0.1299

Correlation of Set Completion Times averaged across all successful trials in the late stage between the Normal and Rotated Conditions was performed to reveal similarity of motor sequence structure. Significant correlations are shown in Red.

Design Matrix example for Paired t-test.

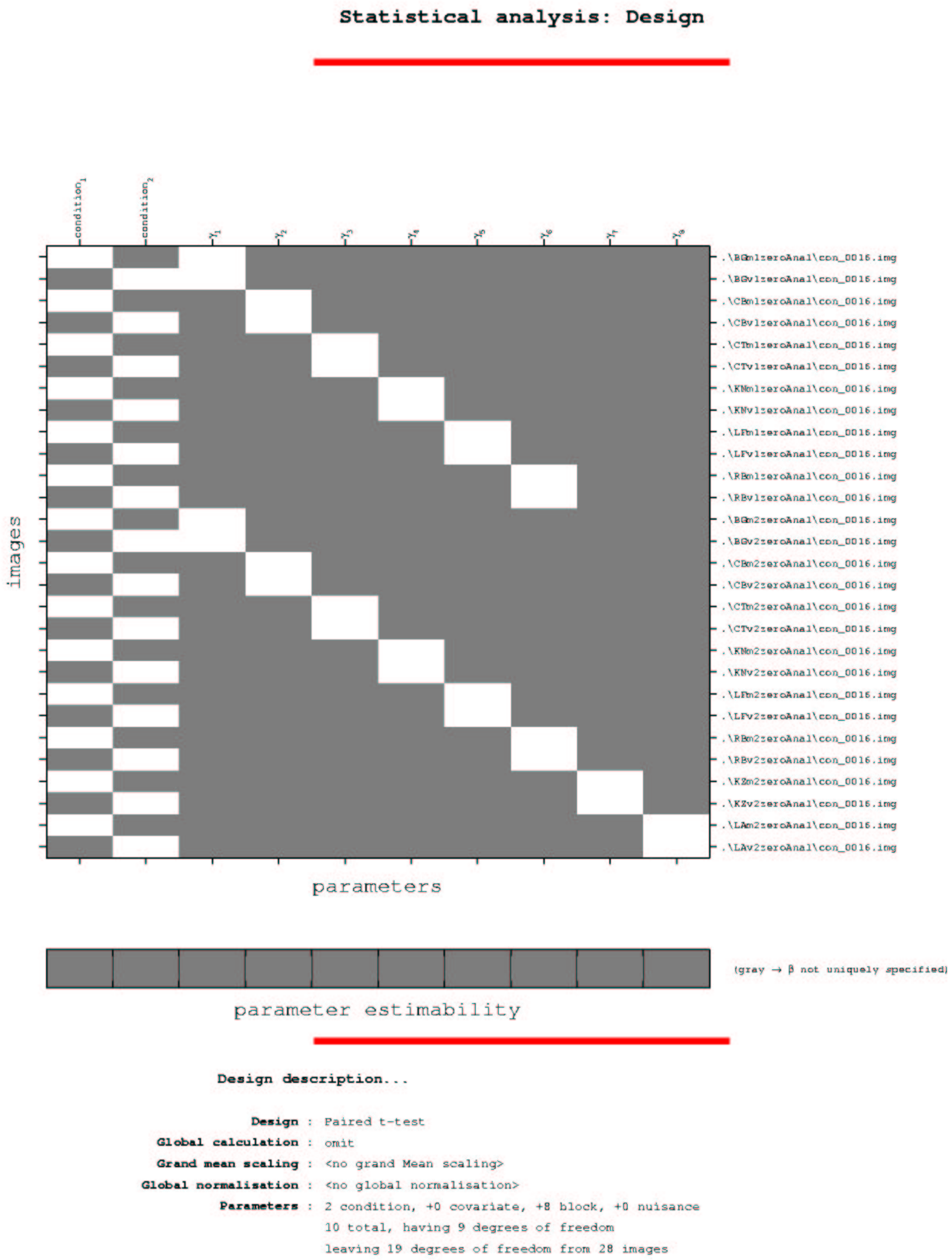

```
Design description...

               Design : Paired t-test
   Global calculation : omit
   Grand mean scaling : <no grand Mean scaling>
Global normalisation : <no global normalisation>
           Parameters : 2 condition, +0 covariate, +8 block, +0 nuisance
                        10 total, having 9 degrees of freedom
                        leaving 19 degrees of freedom from 28 images
```

Figure S3: Group data analysis of fMRI data followed a random effects model as implemented in the SPM99 software. We performed paired t-test between sequence conditions two at a time and allowed for within and between subject variances to be different.

It was observed that the activations in main effects of sequence compared to *follow* in the early and late stages had very large clusters comprising few thousand voxels spanning across several brain areas. We used the Talairach daemon software for counting the number of significant voxels per brain region. As voxel activations were also found in the white matter, we furnish the voxel counts for different search ranges in Table S3. These voxel counts provide a comprehensive overview of the activations found in our tasks.

In the first-level design matrices for individual subjects, we included two behavioural measures (accuracy and response time) as user specified regressors. Table S4 summarises the results of group analysis performed using one sample t-tests at the group level.

Table S3a: Voxel counts for Early Visual-Follow

Brain area ↓ Search Range →		**1 mm**	**3 mm**	**5 mm**	**7 mm**	**9 mm**	**11 mm**
Cerebellum (Culmen)	R	105					
Thalamus (Pulvinar)	R	73	20	0	6	0	0
	L	55	10	6	1	0	0
Caudate Body	R	80	44	65	22	41	6
	L	21	26	27	41	7	11
Ant. Putamen (d)	R	84	55	37	29	1	10
	L	167	44	35	24	2	5
Post. Putamen (d)	R	35	28	57	13	17	5
	L	160	46	65	20	11	0
Globus Pallidus	R	0	0	0	0	0	0
	L	52	15	3	0	0	0
Ventral Striatum	R	0	0	0	0	0	0
	L	98	46	49	3	2	0
Hippocampus	R	6	21	13	13	6	1
	L	0	4	14	9	0	0
Middle temporal gyrus (BA 39)	R	15	18	46	44	19	10
	L	2	3	4	2	8	9
Sup. occipital gyrus (BA 19)	R	16	11	22	2	6	0
	L	8	8	8	0	2	0
Middle occipital gyrus (BA 18/19)	R	3	3	0	2	2	0
	L	17	21	20	23	6	13
Superior Parietal Cortex (BA 7)	R	102	83	51	1	0	0
	L	172	174	71	31	1	9
Inferior Parietal Lobule (BA 40)	R	97	105	80	35	37	7
	L	357	334	119	100	28	43
Precuneus (BA 7)	R	104	109	121	36	8	7
	L	108	140	108	60	18	13
Primary motor (BA 4)	L	15	17	42	9	19	0
Sensory (BA 2/3)	L	146	145	135	76	52	17
Premotor (dorsal) (BA 6)	R	0	6	4	26	11	18
	L	40	60	35	48	44	27
Premotor (ventral) (BA 6)	R	0	2	0	0	8	4
	L	9	24	28	11	27	4
Pre-SMA (BA 6)		0	0	0	0	0	0

Table S3b: Voxel counts for Late Visual-Follow

Brain area ↓ Search Range →		**1 mm**	**3 mm**	**5 mm**	**7 mm**	**9 mm**	**11 mm**
Cerebellum (Culmen)	R	111					
Thalamus (Pulvinar)	R	10	13	3	12	1	0
	L	102	22	22	3	1	0
Caudate Body	R	13	23	41	12	46	5
	L	77	109	64	103	33	87
Ant. Putamen (d)	R	27	29	28	26	1	9
	L	128	59	35	24	2	6
Post. Putamen (d)	R	58	39	55	18	16	5
	L	275	60	64	16	11	5
Globus Pallidus	R	9	1	1	0	0	0
	L	83	12	2	0	0	0
Ventral Striatum	R	53	20	29	1	0	0
	L	68	34	19	3	0	0
Hippocampus	R	21	41	24	18	6	1
	L	0	6	2	13	0	15
Middle temporal gyrus (BA 39)	R	25	26	25	19	18	19
	L	0	9	5	26	10	32
Sup. occipital gyrus (BA 19)	R	16	11	19	2	0	0
	L	0	0	0	0	4	0
Middle occipital gyrus (BA 18/19)	R	10	7	15	5	11	8
	L	14	16	35	30	46	33
Superior Parietal Cortex (BA 7)	R	61	30	29	3	0	0
	L	117	90	39	7	0	0
Inferior Parietal Lobule (BA 40)	R	95	97	56	27	18	3
	L	242	309	116	136	33	65
Precuneus (BA 7)	R	69	60	51	10	0	4
	L	131	160	139	45	18	16
Primary motor (BA 4)	L	22	25	60	15	18	1
Sensory (BA 2/3)	L	166	151	162	94	80	44
Premotor (dorsal) (BA 6)	R	7	35	25	39	19	18
	L	46	71	58	46	58	27
Premotor (ventral) (BA 6)	R	0	0	0	1	0	6
	L	37	70	114	44	97	32
Pre-SMA (BA 6)		13	6	3	0	0	0

Table S3c: Voxel counts for Early Motor-Follow

Brain area ↓ Search Range →		1 mm	3 mm	5 mm	7 mm	9 mm	11 mm
Cerebellum (Culmen)	R	130					
Thalamus (Pulvinar)	R	49	22	21	11	3	0
	L	53	7	32	12	6	5
Caudate Body	R	30	11	26	7	55	11
	L	3	18	15	63	19	49
Ant. Putamen (d)	R	44	38	17	20	0	9
	L	10	7	10	19	2	6
Post. Putamen (d)	R	193	60	52	9	13	5
	L	178	58	53	22	11	5
Globus Pallidus	R	27	5	0	0	0	0
	L	39	12	3	0	0	0
Middle temporal gyrus (BA 39)	R	10	15	58	36	33	23
	L	1	1	9	25	14	49
Sup. occipital gyrus (BA 19)	R	1	0	6	0	1	0
	L	5	5	3	0	7	0
Middle occipital gyrus (BA 18/19)	R	16	30	31	34	13	5
	L	28	43	51	59	51	53
Superior Parietal cortex (BA 7)	R	65	38	32	2	0	0
	L	76	61	40	13	0	6
Inferior Parietal Lobule (BA 40)	R	44	61	45	31	35	13
	L	262	317	103	109	25	47
Precuneus (BA 7)	R	79	18	72	19	6	9
	L	126	167	116	62	14	19
Primary Motor (BA 4)	L	13	14	34	4	7	0
Sensory (BA 2/3)	L	143	150	120	63	63	17
Premotor (dorsal) (BA 6)	R	4	32	16	41	15	22
	L	18	47	42	44	34	27
Premotor (ventral) (BA 6)	R	2	6	12	10	22	34
	L	13	20	24	14	36	4
Middle frontal gyrus (BA 9/46)	R	14	10	16	9	18	13
	L	0	1	2	1	0	0

Table S3d: Voxel counts for Late Motor-Follow

Brain area ↓	**Search Range →**	**1 mm**	**3 mm**	**5 mm**	**7 mm**	**9 mm**	**11 mm**
Cerebellum (Culmen)	R	26					
Thalamus (Pulvinar)	R	0	0	0	0	0	0
	L	2	1	5	0	1	0
Caudate Body	R	7	11	1	0	4	0
	L	12	7	2	11	2	13
Ant. Putamen (d)	R	3	7	4	0	0	0
	L	1	4	2	6	0	0
Post. Putamen (d)	R	5	6	14	7	6	2
	L	45	15	20	4	5	0
Globus Pallidus	R	1	0	0	0	0	0
	L	0	0	0	0	0	0
Middle temporal gyrus (BA 39)	R	0	0	0	0	0	2
	L	0	1	6	3	10	16
Sup. occipital gyrus (BA 19)	R	0	0	0	0	0	0
	L	0	0	0	0	0	0
Middle occipital gyrus (BA 18/19)	R	0	0	0	0	0	0
	L	16	23	28	26	9	13
Superior Parietal cortex (BA 7)	R	47	25	19	2	0	0
	L	98	78	30	6	0	0
Inferior Parietal Lobule (BA 40)	R	23	28	17	7	2	2
	L	289	287	74	80	15	27
Precuneus (BA 7)	R	9	9	15	0	0	0
	L	64	98	65	33	2	7
Primary Motor (BA 4)	L	17	12	18	1	4	0
Sensory (BA 2/3)	L	169	173	97	51	43	23
Premotor (dorsal) (BA 6)	R	12	40	29	43	14	19
	L	45	69	63	45	30	25
Premotor (ventral) (BA 6)	R	0	0	0	0	0	3
	L	63	71	85	28	36	11
Middle frontal gyrus (BA 9/46)	R	0	0	4	9	3	11
	L	26	23	9	4	5	9

Table S4a. Locations of significant BOLD signal in the *visual* regressor (Accuracy)

			Activation				Deactivation			
Brain area		BA	Coordinates (mm)			*T* value	Coordinates (mm)			*T* value
			x	y	z		x	Y	z	
Cerebellum										
Ant. Lobe (Culmen)	R			---			12	-63	-10	5.34
Basal Ganglia										
Caudate Head	L			---			-8	16	1	4.90
Caudate Body	R			---			10	3	15	5.30
	L			---			-14	-20	25	5.26
Ant. Putamen (d)	R			---			18	3	15	4.14
Post. Putamen (d)	L			---			-26	-2	0	6.58
Hippocampus	R			---			30	-33	-3	4.08
	L			---				---		
Sup. occipital gyrus	R	19	36	-78	32	5.27		---		
Middle occipital gyrus	R	19	44	-85	8	5.60		---		
	L	19	-36	-83	13	4.30		---		
Parietal cortex										
Superior	R	7	34	-58	51	6.35		---		
Posterior	R	7	18	-60	38	5.68		---		
	L	7	-12	-70	42	7.33		---		
Precuneus	L	7	-8	-51	58	4.84		---		
Inferior Lobule	R	40		---			59	-43	43	5.95
	L	40		---			-53	-54	43	4.48
Sensory	L	2		---			-48	-21	47	4.18
Primary motor	L	4		---			-44	-15	49	3.95*
Cingulate Gyrus		32	4	21	32	6.95		---		
Inferior frontal gyrus	L	45	-46	29	0	5.11		---		
	L	10	-42	49	1	4.99		---		
Middle frontal gyrus	L	9		---			-34	36	29	4.56
Medial frontal gyrus		10		---			-6	49	7	4.81

Stereotaxic Talairach coordinates of peak activation obtained with $p < .001$ (uncorrected). Abbreviations: Sup. Superior, Inf. Inferior, d Dorsal, Ant. Anterior, Post. Posterior. *indicates the coordinate where a brain–behavior correlation analysis was performed.

Table S4b. Locations of significant BOLD signal in the *visual* regressor (Time)

			Activation				Deactivation			
Brain area		BA	Coordinates (mm)			*T* value	Coordinates (mm)			*T* value
			x	y	z		x	y	z	
Cerebellum										
Post. Lobe (Declive)	R			---			14	-57	-11	6.27*
Basal Ganglia										
Caudate Body	R			---			18	16	5	4.22
Ant. Putamen (d)	R			---			28	2	4	4.03
	L			---			-30	4	2	4.16
Parietal cortex										
Posterior	R	7	14	-58	42	5.44		---		
Inferior Lobule	L	40	-34	-54	40	4.76		---		
Primary motor	L	4		---			-42	-15	45	5.61
Post. Cingulate		31	-18	-63	16	8.02		---		
Pre-SMA		6		---			-4	8	46	4.15*
Premotor (dorsal)	L	6		---			-30	-6	39	4.46*
Middle frontal gyrus	R	46		---			46	30	21	5.04*
Sup. frontal gyrus	R	10		---			22	49	18	4.20

Stereotaxic Talairach coordinates of peak activation obtained with $p < .001$ (uncorrected). Abbreviations: Sup. Superior, d Dorsal, Ant. Anterior, Post. Posterior, SMA Supplementary Motor Area, *indicates the coordinate where a brain–behavior correlation analysis was performed.

Table S4c. Locations of significant BOLD signal in the *motor* regressor (Accuracy)

			Activation				Deactivation			
Brain area		BA	Coordinates (mm)			*T* value	Coordinates (mm)			*T* value
			x	y	z		x	y	z	
Basal Ganglia										
Caudate Body	R			---			12	8	7	6.77
Inferior occipital gyrus	R	18	38	-84	-3	5.92		---		
Middle occipital gyrus	L	18/19	-30	-89	8	5.91		---		
Parietal cortex										
Precuneus	R	7	4	-58	51	5.29*		---		
	L	7	-6	-63	51	4.14*		---		
Post. Cingulate		30	14	-60	12	5.60				
SMA		6		---			-6	-17	49	4.21*
Middle frontal gyrus	R	46		---			44	30	19	4.69
	L	46		---			-44	25	25	4.75

Stereotaxic Talairach coordinates of peak activation obtained with $p < .001$ (uncorrected). Abbreviations: Post. Posterior, SMA Supplementary Motor Area. *indicates the coordinate where a brain–behavior correlation analysis was performed.

Table S4d. Locations of significant BOLD signal in the *motor* regressor (Time)

			Activation				Deactivation			
Brain area		BA	Coordinates (mm)			*T* value	Coordinates (mm)			*T* value
			x	y	z		x	y	z	
Cerebellum										
Ant. Lobe (Culmen)	R			---			10	-65	-9	4.30
Middle temporal gyrus	L	39	-36	-65	27	4.47		---		
Parietal cortex										
Posterior	L	7	-14	-66	49	4.24		---		
Ant. Cingulate		24/32	-4	30	10	5.28		---		

Stereotaxic Talairach coordinates of peak activation obtained with $p < .001$ (uncorrected). Abbreviations: Ant. Anterior

Brain areas and sequencing processes.

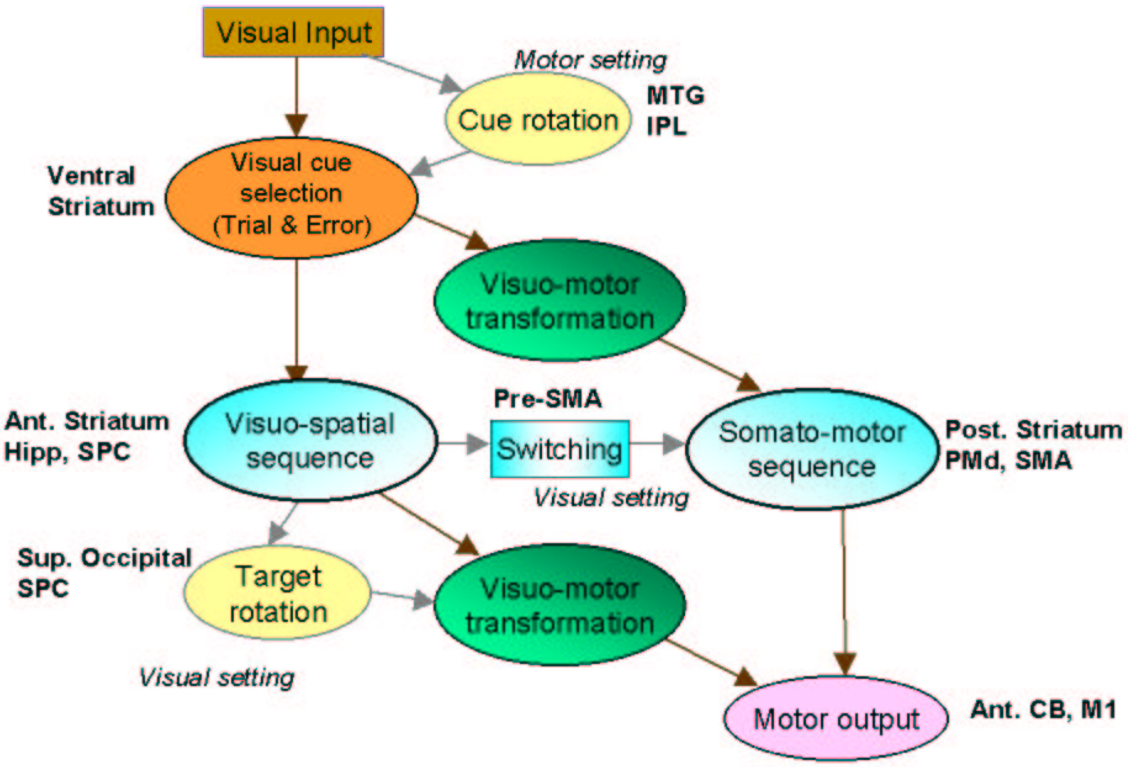

Figure S4: A visual cue is selected by trial and error from the visual inputs and motor output is generated after an appropriate visuo-motor transformation. The visual cues and motor responses that are processed sequentially are stored in the representational buffers depicted as visuo-spatial sequence and somato-motor sequence, respectively. Once representations are learned, they can guide the performance directly without resorting to the selection process. Based on observations in previous studies involving trial and error learning (Jenkins et al., 1994; Jueptner et al., 1997b), sustained activity observed in the ventral striatum in both the early and late stages of *visual* setting may be attributed to the trial and error process adopted for cue selection. Interestingly, when there was no emphasis on cue selection process as in the *motor* setting, ventral striatal activity was absent. Activity found in the *rotated* > *normal* contrasts would reveal areas related to rotational transformations. Activity observed in the superior occipital gyrus and superior parietal cortex in the *visual* > *normal* contrast may support processes involved in target rotation and the activity in the middle temporal gyrus and inferior parietal cortex in the *motor* > *normal* contrast may be related to the processes involved in cue rotation. In the visual-normal experiments subjects used the same visuo-spatial sequence but learned two motor sequences, one corresponding to the *normal* and the other to *visual* setting. We suggest that the pre-Supplementary Motor Area (Pre-SMA) may have a role in learning new sequence and also in sequence switching (Shima et al., 1996). Anterior cerebellum is engaged in the optimization of movement parameter and timing information required for motor execution mediated by the Primary Motor Cortex (M1). We suggest that as sequence learning progresses from the early to the late stage, visuo-spatial sequence representation gets established in anterior striatum, superior parietal cortex (SPC) and the hippocampus whereas somato-motor sequence representation is encoded in the posterior striatum, dorsal premotor (PMd) and supplementary motor area (SMA). Abbreviations: Ant. Anterior, Post. Posterior. MTG: Middle Temporal Gyrus, IPL: Inferior Parietal Lobe